Euro. Jnl of Applied Mathematics (2001), *vol.* 12, *pp.* 253–291. Printed in the United Kingdom

Stability of compressive and undercompressive thin film travelling waves

ANDREA L. BERTOZZI[1]†, ANDREAS MÜNCH[2], MICHAEL SHEARER[3]‡ and KEVIN ZUMBRUN[4]§

[1] *Center for Nonlinear and Complex Systems, and Departments of Mathematics and Physics, Duke University, Durham, NC 27708-0320, USA*
[2] *Zentrum Mathematik (H4), Technische Universität München, D-80290 München, Germany*
[3] *Center for Research in Scientific Computation, and Department of Mathematics, North Carolina State University, Raleigh, NC 27695–8205, USA*
[4] *Department of Mathematics, Indiana University, Bloomington, IN 47405-4301, USA*

(*Received 27 January 2000; revised 19 December 2000*)

Recent studies of liquid films driven by competing forces due to surface tension gradients and gravity reveal that undercompressive travelling waves play an important role in the dynamics when the competing forces are comparable. In this paper, we provide a theoretical framework for assessing the spectral stability of compressive and undercompressive travelling waves in thin film models. Associated with the linear stability problem is an Evans function which vanishes precisely at eigenvalues of the linearized operator. The structure of an index related to the Evans function explains computational results for stability of compressive waves. A new formula for the index in the undercompressive case yields results consistent with stability. In considering stability of undercompressive waves to transverse perturbations, there is an apparent inconsistency between long-wave asymptotics of the largest eigenvalue and its actual behaviour. We show that this paradox is due to the unusual structure of the eigenfunctions and we construct a revised long-wave asymptotics. We conclude with numerical computations of the largest eigenvalue, comparisons with the asymptotic results, and several open problems associated with our findings.

1 Introduction

Driven films exhibit a variety of complicated dynamics ranging from rivulets and saw-tooth patterns in gravity driven flows [JdB92, SV85] to patterns in spin coating [FH94] and surfactant driven films [TWS89]. A theoretical framework for these problems is provided by a lubrication approximation of the Navier–Stokes equations [MW99, Gre78]. This yields a single partial differential equation for the film thickness as a function of position on the solid substrate and time.

† Supported by Office of Naval Research grant N00014-96-1-0656, National Science Foundation grants DMS-0074049 and DMS-9983320, and a Sloan Research Fellowship.

‡ Adjunct Professor of Mathematics at Duke University. Research supported by National Science Foundation grant DMS-9818900 and by Army Research Office grant DAAG55-98-1-0128.

§ Research supported in part by the National Science Foundation under Grant No. DMS-9706842.

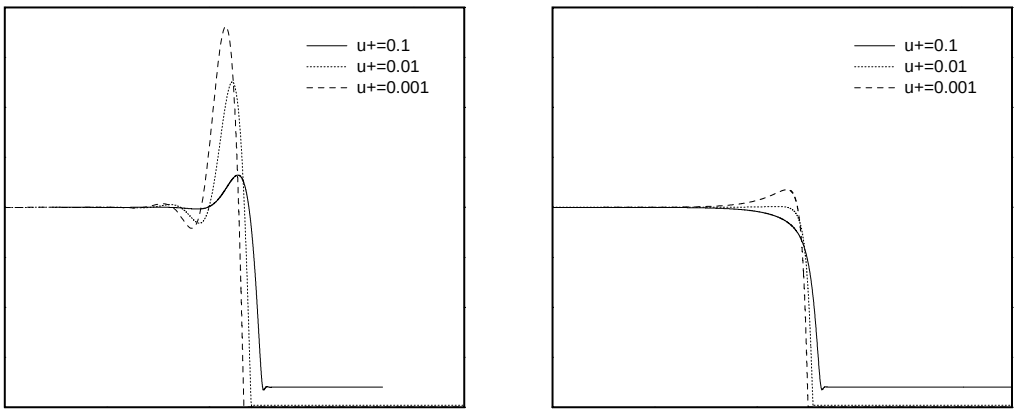

(a) (b)

FIGURE 1. Compressive travelling waves for the flux $f(u) = u^3$, connecting $u_- = 1$ to u_+, for three values of u_+. (a) $\beta = 0$, $\gamma = 1$. All waves are linearly unstable to transverse perturbations. (b) $\beta = 5$, $\gamma = 1$. The waves with $u_+ = 0.1$, 0.01 are linearly stable to transverse perturbations.

For directionally driven films, the driving force enters into the lubrication approximation as the flux f in a scalar hyperbolic conservation law $u_t + (f(u))_x = 0$. Here $u > 0$ is the film thickness and x is the direction of the driving force. For *gravity* driven flow on an incline, the tangential component of gravity yields a flux proportional to u^3 [Hup82]. For *surface-tension gradient* driven flows f is proportional to u^2 [CHTC90]. In each of these cases, the flux is convex. Consequently, driven fronts in the film correspond to *compressive shock* solutions, whose simplest form is

$$u(x,t) = \begin{cases} u_-, & \text{if} \quad x < st, \\ u_+, & \text{if} \quad x > st, \end{cases} \tag{1.1}$$

in which the shock speed $s = (f(u_-) - f(u_+))/(u_- - u_+)$ satisfies the entropy condition

$$f'(u_+) < s < f'(u_-); \tag{1.2}$$

equivalently, characteristics enter the shock on each side. Small variations in height near a compressive shock are propagated towards the shock from both sides.

In practice, the discontinuous fronts (1.1) are smoothed by diffusive effects, primarily through surface tension. In the lubrication approximation, surface tension appears as a fourth order nonlinear regularization of the conservation law, but there is also second-order nonlinear diffusion induced by the component of gravity normal to the incline, leading to the equation

$$u_t + (f(u))_x = -\gamma \nabla \cdot (u^3 \nabla \Delta u) + \beta \nabla \cdot (u^3 \nabla u). \tag{1.3}$$

In this equation, $\gamma > 0$ and $\beta \geqslant 0$ are constants. The shock waves (1.1) correspond to smooth travelling wave solutions of (1.3); for small $\beta \geqslant 0$, they typically have oscillatory overshoots and undershoots on either side of the shock. Additionally, the nonlinearity in the fourth order diffusion causes a single very pronounced overshoot or 'bump' on the leading edge of the shock (see Figure 1a); this structure is often referred to as a *capillary ridge* in experiments. Capillary ridges produced by surface tension are well known to

be linearly unstable to long-wave perturbations in the transverse direction of the flow, producing the well-known *fingering instability* [CC92, THSJ89, KT97, YC99]. The effect of larger β is to suppress the bump (see Figure 1b). The disappearance of the bump (for β sufficiently large) is accompanied by a transverse stabilization of the wave [BB97].

Experiments with doubly driven film flow, in which gravitational and surface tension gradient stresses are competing, have uncovered some new phenomena. While very thin films produce the characteristic capillary ridge followed by a fingering instability [CHTC90], thicker films produce a wider capillary ridge that continues to broaden. Furthermore, the front, or leading edge of the film, remains planar; it does not experience fingering [BMFC98, KT98].

The lubrication approximation for this problem yields an equation of the form (1.3) with a non-convex flux (see references listed above and below)

$$f(u) = u^2 - u^3. \tag{1.4}$$

Numerical experiments [BMS99, MB99, M99] and analysis [BS99] with β small show that the experimental observations can be explained by the presence of *undercompressive shocks*. In particular, while weak jump initial data give rise to compressive waves, moderately strong jumps can evolve into a double shock structure in which the leading shock is undercompressive: it has the form (1.1) with a shock speed s that is larger than the characteristic speeds $f'(u_\pm)$, and hence violates the entropy condition (1.2). The trailing wave is compressive (satisfying (1.2)) and travels at a slower speed. For stronger initial jumps, the solution evolves as a rarefaction wave connected to an undercompressive wave [MB99]; this structure explains discrepancies between earlier thin film experiments [LL] and analysis based on the classical theory of conservation laws, which considers only compressive waves. The presence of undercompressive shocks is due to the combined effects of the non-convex flux and the fourth order diffusion. Moreover, numerical computations [MB99] confirm that the undercompressive leading wave is linearly stable to transverse perturbations, while the stability of the compressive shocks depends on the absence of a capillary ridge.

The numerical simulations of [BMS99] also reveal a complicated relationship between initial condition/far field boundary condition and asymptotic behaviour of solutions. More specifically, for a range of far-field boundary conditions, there are multiple stable long-time asymptotic solutions including a number of compressive travelling waves (e.g. see Figure 2) and the two-wave structure described above, with an undercompressive leading front. The specific asymptotic solution that emerges in this case depends upon the shape of the initial data $u(x,0)$. For other far-field boundary conditions, only the two-wave structure is realized in the long-time limit, irrespective of the shape of the initial data. A detailed explanation of this behaviour is provided in [BMS99].

In this paper, we specifically focus on the stability theory for travelling wave solutions $u(x,y,t) = \bar{u}(x-st)$ of the general equation

$$u_t + f(u)_x = \nabla\cdot(b(u)\nabla u) - \nabla\cdot(c(u)\nabla\Delta u), \tag{1.5}$$

in which we assume (on the range of u considered)

(H_0) $f, b, c \in C^2$,

(H_1) $c \geqslant \eta > 0, \quad b \geqslant 0$

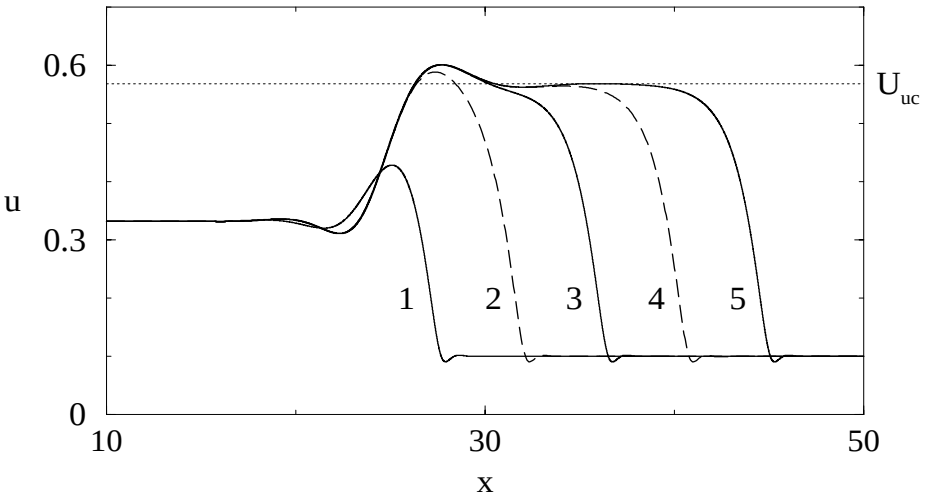

FIGURE 2. Compressive travelling waves for (1.6) with $\beta = 0$ and $\gamma = 1$, connecting $u_- \approx 0.332051$ to $u_+ = 0.1$. Waves numbered 1, 3 and 5 are numerically stable in one space dimension, while waves 2 and 4 are unstable. All waves are unstable to multidimensional perturbations. For this special value of u_- there are an infinite number of compressive waves connecting to u_+.

while keeping in mind the special case studied in [BMS99], corresponding to:

$$f(u) = u^2 - u^3, \quad b(u) = \beta u^3, \quad c(u) = \gamma u^3, \quad \beta \geqslant 0, \gamma > 0. \tag{1.6}$$

The condition (H_1) ensures that equation (1.5) is nonsingular.[1] As we will show, slightly different methods are required to analyze compressive versus undercompressive waves.

The existence of travelling waves is itself an interesting problem. For convex fluxes, the existence of travelling waves can be proved by a shooting argument as in [KH75] or using topological methods involving the Conley index as in [Ren96, BMS99]. The case of a non-convex flux such as (1.4) is more complicated. In particular, the phase portrait for the resulting travelling wave ODE can have more than two equilibria and the possibility of multiple heteroclinic orbits, including those that correspond to undercompressive travelling waves. A recent proof of existence of undercompressive waves for the case (1.5), (1.6) with sufficiently small $D = \beta/\gamma^{1/3} \geqslant 0$ was given in [BS99]. Moreover, non-existence of undercompressive waves for large D was also established. Numerical results exploring the effect of varying D over a large range are explored in [M99].

In this paper, we focus on issues concerning the *stability* of travelling wave solutions of (1.5). In § 2, we consider stability to one-dimensional perturbations, and in §§ 3 and 4 we consider multidimensional stability.

A stability theory based on the Evans function [E, AGJ1, PW] has been developed for the stability analysis of general travelling waves. These ideas have recently been extended to the study of viscous shock waves in systems of conservation laws with second-order

[1] Note that for the nonlinear problem, there is an inherent singularity at $u = 0$. Moreover, an *a priori* positive lower bound for the solution of the nonlinear problem is generally not available. However, in this paper the nonlinear equation is linearized about a positive solution (a travelling wave); the resulting linear equation is not singular.

diffusion [GZ, ZH] and in scalar conservation laws with second-order diffusion and third-order dispersion [D, HZ.2, Z.3]. Undercompressive waves arise in both cases. In this paper, we use the Evans function to understand linear stability of travelling waves of the scalar equation (1.5). For this problem, undercompressive waves are generated from the non-convex flux and fourth order diffusion. This new context raises novel technical issues in using the Evans function. Moreover the complex structure of the travelling wave problem has interesting ramifications for the study of stability.

In § 2, following the general approach of [GZ], we find a formula for an index Γ related to the Evans function. When Γ is negative, the travelling wave is unstable, since the presence of a positive growth rate is predicted. When positive, the index is consistent with stability. (The index only predicts the parity of the number of unstable eigenvalues or positive growth rates; when the index is positive, we are assured only that there are an even number of unstable eigenvalues, not that there are none.) The geometry underlying this index is used in § 2 to explain the following numerically observed feature: when there are multiple compressive waves for the same upstream and downstream thicknesses, the waves come in pairs, one stable and one unstable to one-dimensional perturbations. An interesting open problem is to give a rigorous proof of *stability*. Such a proof would require further bounds on potential unstable eigenvalues (perhaps by a variant of Grillakis' method, as in [PW, AGJS, D, P]).

For undercompressive waves, the index requires special treatment due to the behaviour of eigenfunctions associated with the linearization about the travelling wave. In this case we derive a new simple expression for the index that we calculate easily from pictures of numerical results. This reduction turns out to be necessary for practical evaluation of the Evans function index in the case of travelling waves for higher order problems. It is a refinement of the general theory developed in [D, GZ] and directly extends to arbitrary order *systems*.

The difference between the compressive and undercompressive cases appears even more forcefully in the consideration of multidimensional stability. In § 3, we outline the framework for a study of stability to two-dimensional perturbations. We focus on long-wave perturbations, and show numerically in § 4 that compressive waves are unstable, in agreement with long-wave asymptotics developed in § 3 (and also in [BB97, KT98]). However, when considering undercompressive waves, there is a mathematical puzzle we call the *long-wave paradox*: a formal calculation [KT98, BB97] of the low-frequency (long-wave) expansion of the growth rate of fingering perturbations as a function of spatial frequency yields an explicit formula for the leading order asymptotics of the growth rate of perturbations at long wave lengths. While this asymptotic formula agrees well with computed eigenvalues in the case of compressive waves, it fails for undercompressive waves. In § 3 we resolve the long-wave paradox by showing how, for undercompressive waves, the formal calculation overlooks an interesting feature of the linearized problem. In § 4, the resolution of the long-wave paradox is used to interpret numerical calculations of growth rates, demonstrating that undercompressive waves are stable to transverse perturbations.

In § 4, we also identify a curious feature of the growth rates. For parameter values for which there is an undercompressive wave, there are also multiple travelling waves and, moreover, the double shock structure collapses; the trailing compressive wave and the

leading undercompressive wave have the same speed. The graphs of the growth rates (as a function of wave number) for the (unstable) compressive waves approach the maximum of the growth rates for the undercompressive wave and the compressive trailing wave. We interpret this observation in terms of the linearized equation, by observing that the trajectories of the compressive travelling waves approach a combination of the trajectories for the undercompressive wave and the trailing compressive wave.

2 The one dimensional case

To begin with, we consider solutions $u = u(x,t)$ of equation (1.5) that are independent of y:

$$u_t + f(u)_x = (b(u)u_x)_x - (c(u)u_{xxx})_x. \tag{2.1}$$

Suppose there is a travelling wave solution, which (by adding a linear term to f, $f(y) = \tilde{f}(y) - sy$) we may take to be stationary:

$$u(x,t) = \bar{u}(x). \tag{2.2}$$

Then $u = \bar{u}(x)$ satisfies the travelling wave ODE

$$c(u)u''' = b(u)u' - (f(u) - f(u_+)) \tag{2.3}$$

and boundary conditions

$$\lim_{x\to\pm\infty} \bar{u}(x) = u_\pm. \tag{2.4}$$

In addition to the standing assumptions (H_0), (H_1), we assume standard nondegeneracy conditions from [ZH][2]:

(H_2) $a_\pm := f'(u_\pm) \neq 0$.

(H_3) Solutions of (2.3)–(2.4) are (locally to $\bar{u}$) unique up to translation.

Remark (H_2) holds if and only if $(u_\pm, 0, 0)$ are hyperbolic rest points of the first-order system (for u, u', u'') associated with (2.3). Equivalently, it states that that the wave speed is non-characteristic for the underlying conservation law $u_t + (f(u))_x = 0$.

Linearizing (2.1) about $\bar{u}(\cdot)$ gives

$$v_t = Lv := -(cv_{xxx})_x + (bv_x)_x - (av)_x,$$

in which $c = c(\bar{u}(x))$, $b = b(\bar{u}(x))$, $a = f'(\bar{u}(x)) - b'(\bar{u})\bar{u}_x + c'(\bar{u})\bar{u}_{xxx}$.

Letting $v(x,t) = e^{\lambda t}w(x)$, we obtain the eigenvalue problem $Lw = \lambda w$:

$$-(cw''')' + (bw')' - (aw)' = \lambda w. \tag{2.5}$$

Here, and below, $'$ denotes differentiation with respect to x.

To demonstrate linear stability of the travelling wave $\bar{u}$, we want to show that if $\mathrm{Re}\,\lambda \geqslant 0, \lambda \neq 0$, then equation (2.5), with suitable boundary conditions at $\pm\infty$, has only the trivial solution $w \equiv 0$. Our approach to this question is through the Evans function $D(\lambda)$ (defined below) of [AGJS, GZ]. This is an analytic function whose zeroes in the right

[2] (H_3) is the specialization to the scalar case of the more general (H_3) in [ZH].

half plane (minus the exceptional point $\lambda = 0$, which lies on the boundary of the essential spectrum) correspond precisely to eigenvalues of L. Moreover, as shown in [ZH, HZ.2], stability under quite general circumstances is equivalent to the condition:

($\mathscr{D}$) $D(\cdot)$ has precisely one zero on $\{\mathrm{Re}(\lambda) \geqslant 0\}$, consisting of a simple root at $\lambda = 0$.

The Evans function itself is rather difficult to evaluate; a more readily computable quantity is the *stability index* [J, PW, GZ, Z.2, Z.3]

$$\Gamma := \operatorname{sgn} D'(0) \lim_{\lambda \longrightarrow \infty} \operatorname{sgn} D(\lambda), \tag{2.6}$$

where the limit is along the real axis. This quantity, taking values $\Gamma = \pm 1$, gives the parity of the number of zeroes of $D(\cdot)$ in the unstable half-plane $\mathrm{Re}\,\lambda > 0$. This follows from the observations that (i) Γ records the number of crossings of $D(\lambda)$ through zero as λ moves along the positive real axis, and (ii) non-real zeroes of D appear in conjugate pairs, since L is real. In particular, $\Gamma = -1$ implies instability of the travelling wave, whereas $\Gamma = 1$ is consistent with stability. It is this computable index, and its interpretation in terms of the phase portrait of the travelling wave ODE, that provides much of the theoretical explanation of the numerically observed stability phenomena.

To construct the Evans function, we explore solutions of (2.5) as follows. Since the equation is fourth order, for each λ, there will be a four dimensional set of solutions. For $\lambda \in \{\mathrm{Re}(\lambda) \geqslant 0\}/\{0\}$, we can choose a basis for the subspace $\mathscr{S}^+$ of solutions that approach zero as $x \longrightarrow \infty$ and a basis for the subspace $\mathscr{U}^-$ of solutions that approach zero as $x \longrightarrow -\infty$. Then λ is an eigenvalue if $\mathscr{S}^+$ and $\mathscr{U}^-$ have non-trivial intersection. That is, we need a condition for the intersection of two linear subspaces of functions. This condition is that the Evans function $D(\lambda)$, defined to be the Wronskian of the two pairs of basis functions of $\mathscr{S}^+$ and $\mathscr{U}^-$, should vanish. In the present situation, the sign of the Wronskian is shown to be independent of x. The construction of the Evans function extends analytically to $\lambda = 0$, a fact that we use later in this section to compute the stability index.

In the construction of $D(\lambda)$, we do not need to include information about whether the underlying travelling wave is compressive or undercompressive. After the Evans function is defined and related to stability of travelling waves, we then focus on the compressive and undercompressive cases in turn. In §§ 2.5 and 2.6, we show that these cases differ most significantly at $\lambda = 0$, due to the fact that small disturbances propagate through an undercompressive wave, rather than being absorbed, as they are for a compressive wave. This distinction reveals itself in the structure of the subspaces $\mathscr{S}^+$ and $\mathscr{U}^-$, but it can already be seen in the behaviour at $x = \pm\infty$, which we now discuss.

2.1 Asymptotic eigenvalue equations

As $x \to \pm\infty$, behaviour of (2.5) is governed by the asymptotic constant coefficient equations

$$c_\pm w'''' = b_\pm w'' - a_\pm w' - \lambda w. \tag{2.7}$$

Here and below, we use subscripts $\pm$ to indicate that quantities depending on u are evaluated at $u = \bar{u}(\pm\infty)$, respectively (e.g. $c_+ = c(\bar{u}(\infty))$. In particular, $a_\pm = f'(u_\pm)$, so that

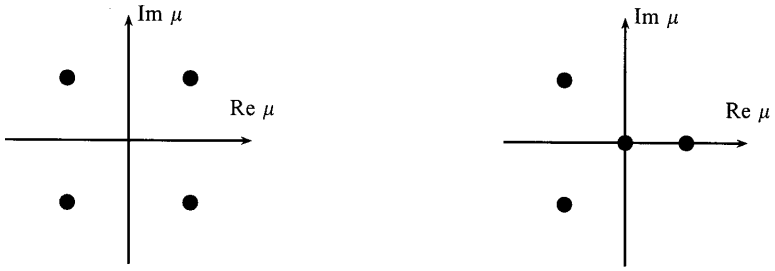

(a) $\lambda \to +\infty$ (b) $\lambda = 0$, $b_\pm = 0$, $a_\pm < 0$

FIGURE 3. Roots of equation (2.8).

the sign of $a_\pm$ governs whether characteristics for the underlying conservation law point towards the stationary front, or away from the front. This distinction shows the effect of the conservation law on the direction of propagation of small disturbances.

The normal modes $w := e^{\mu_j^\pm x}$ of (2.7) are determined by the characteristic equation

$$c_\pm \mu^4 - b_\pm \mu^2 + a_\pm \mu + \lambda = 0. \tag{2.8}$$

First note that for $\lambda = 0$, one of the roots is $\mu = 0$. This corresponds to the constant solution of equation (2.7) when $\lambda = 0$. For $\lambda \neq 0$, we find that all solutions of (2.8) have nonzero real part.

Recall that we need to distinguish solutions $w(x)$ that decay at $x = +\infty$, for which $\mathrm{Re}(\mu) < 0$ (termed *stable* in Lemma 2.1 below) and solutions $w(x)$ that decay at $x = -\infty$, for which $\mathrm{Re}(\mu) > 0$ (termed *unstable* in Lemma 2.1).

Lemma 2.1 *For $\lambda \in \{\mathrm{Re}(\lambda) \geqslant 0\}/\{0\}$, (2.7) has two* **stable** *(i.e. negative real part) and two* **unstable** *roots, $\mu_1, \mu_2 < 0 < \mu_3, \mu_4$ (ordering by real parts). At $\lambda = 0$, there are two cases:*

$$\begin{aligned} (a_\pm > 0): &\quad \mu_1 < \mu_2 = 0 < \mu_3, \mu_4. \\ (a_\pm < 0): &\quad \mu_1, \mu_2 < 0 = \mu_3 < \mu_4. \end{aligned}$$

Proof ($\lambda \neq 0$): First, observe that (2.8) has no imaginary roots μ for $\lambda \in \{\mathrm{Re}(\lambda) \geqslant 0\} \setminus \{0\}$. For, setting $\mu = ki$ in (2.8), we have the dispersion relation

$$\lambda = -a_\pm ik - b_\pm k^2 - c_\pm k^4, \tag{2.9}$$

giving $\mathrm{Re}(\lambda) < 0$ unless $k = 0$. Thus, the number of stable/unstable roots is constant. Taking $\lambda \to +\infty$, on the real axis, we have $\mu \sim (-\lambda)^{1/4} = |\lambda|^{1/4}(-1)^{1/4}$, giving two stable and two unstable roots (Figure 3(a)).

($\lambda = 0$): At $\lambda = 0$, we can factor (2.8) as

$$c_\pm \mu^3 - b_\pm \mu + a_\pm = 0, \qquad \mu = 0. \tag{2.10}$$

Clearly, the first equation has no imaginary roots for $a_\pm \neq 0$, so, we can again count roots by homotopy, taking $b_\pm \to 0$ to find $\mu = \left(-\frac{a_\pm}{c_\pm}\right)^{1/3}$. This gives two stable roots and

one unstable root for $a_\pm < 0$, together with $\mu = 0$, as claimed (Figure 3(b)). The case $a_\pm > 0$ is symmetric. □

Now write (2.7) as a first order system

$$W' = \mathbb{A}_\pm(\lambda)W, \qquad \mathbb{A}_\pm := \begin{pmatrix} 0 & 1 & 0 & 0 \\ 0 & 0 & 1 & 0 \\ 0 & 0 & 0 & 1 \\ -\lambda/c & -a/c & b/c & 0 \end{pmatrix}_\pm \tag{2.11}$$

in the phase variable $W := (w, w', w'', w''')^t$. Throughout this paper, we will identify solutions of such fourth order scalar ODEs with solutions of their corresponding first order system.

For $\lambda \neq 0$, each root μ_k is associated with an eigenfunction $w(x) = e^{\mu_k x}$, a solution of (2.7). Then $W := (w, w', w'', w''')^t$ is a solution of (2.11). Since the equation is linear, these exponential solutions can be combined linearly to form subspaces of solutions. In keeping with the strategy of distinguishing exponentially decaying from exponentially growing solutions, we separate the corresponding subspaces of solutions $\overline{\mathscr{S}}^+, \overline{\mathscr{U}}^-$, where $\overline{\mathscr{S}}^+$ is the two-dimensional invariant subspace of solutions that decay as $x \longrightarrow \infty$, and $\overline{\mathscr{U}}^-$ is the two-dimensional invariant subspace of solutions that decay as $x \longrightarrow -\infty$. The content of the following corollary is that not only are these subspaces two dimensional for $\lambda \neq 0, Re(\lambda) \geqslant 0$, but they also extend analytically to $\lambda = 0$ as two dimensional subspaces, even though for $\lambda = 0$ each subspace may have a non-decaying eigenfunction (depending on the sign of $a_\pm$) as described in Lemma 2.1.

In the case of a compressive wave, $a_- > 0$ and $a_+ < 0$. Thus for $\lambda = 0$ both $\overline{\mathscr{S}}^+$ and $\overline{\mathscr{U}}^-$ are composed of decaying eigenfunctions at their respective infinities in x. On the other hand, for an undercompressive wave, a_- and a_+ have the same sign. If they are both negative then for $\lambda = 0$, $\overline{\mathscr{U}}^-$ has one nondecaying eigenfunction at $x \to -\infty$ while $\overline{\mathscr{S}}^+$ has two decaying modes at ∞. This difference between undercompressive and compressive waves carries over to the non-constant coefficient case describing the full eigenvalue problem (2.5). Consequently, in calculating the index Γ we treat the compressive and undercompressive cases separately.

Corollary 2.2 *The stable/unstable subspaces $\overline{\mathscr{S}}^+/\overline{\mathscr{U}}^-$ associated with $\mathbb{A}_\pm(\cdot)$ are each two-dimensional on $\{\mathrm{Re}(\lambda) \geqslant 0\}/\{0\}$, and extend* **analytically in** *λ to $\{\mathrm{Re}\,\lambda \geqslant 0\}$. More precisely, there exist bases $\{V_1^+, V_2^+\}, \{V_3^-, V_4^-\}$ for the subspaces $\overline{\mathscr{S}}^+, \overline{\mathscr{U}}^-$:*

$$\overline{\mathscr{S}}^+ = \mathrm{span}\{V_1^+, V_2^+\}, \tag{2.12}$$

$$\overline{\mathscr{U}}^- = \mathrm{span}\{V_3^-, V_4^-\}. \tag{2.13}$$

The bases can be chosen to depend analytically on λ and have the symmetry $V_j^\pm(\bar{\lambda}) = \overline{V_j^\pm(\lambda)}$.

Proof The dimension follows from Lemma 2.1. Likewise, since groups μ_1, μ_2 and μ_3, μ_4 remain spectrally separated on $\{\mathrm{Re}\,\lambda \geqslant 0\}$, the generalized eigenprojections onto their associated subspaces are each analytic, by standard matrix perturbation theory [K]. The eigenprojections are given by the resolvent formula $P := \int_\Gamma (\mathbb{A}_\pm - \mu I)^{-1} d\mu$, Γ a contour enclosing $\mu_1^\pm$, $\mu_2^\pm$ (resp. $\mu_3^\pm$, $\mu_4^\pm$). If Γ is chosen to be symmetric with respect to complex

conjugation, then P is as well, by the corresponding property of $\mathbb{A}_\pm$. Choosing an analytic basis of eigenvectors by the construction of [K, pp. 99–102], we retain the above symmetry. □

2.2 Stable and unstable manifolds

In the previous subsection, we froze the coefficients in the ODE (2.5), by setting $u = u_+$ and $u = u_-$. This allows us to capture the behaviour of solutions of the nonconstant coefficient equation (2.5) as $x \longrightarrow \pm\infty$.

Given a solution $\varphi(x)$ of (2.5), we associate with it the vector of derivatives $\Phi(x) = (\varphi(x), \varphi'(x), \varphi''(x), \varphi'''(x))^t$. Given such a vector Φ, the angle it makes with a subspace $\mathscr{T}$ of the four dimensional phase space is the minimum of the angle between Φ and all vectors in $\mathscr{T}$.

On $\{\mathrm{Re}\,\lambda \geqslant 0\}$, define $\mathscr{S}^+$ to be the subspace of solutions φ of the variable coefficient equation (2.5) whose corresponding vectors Φ approach, in angle, the subspace $\bar{\mathscr{S}}^+$ of solutions of the constant coefficient problem as $x \to +\infty$ (Note that the bar distiguishes the constant coefficient problem as $x \to \pm\infty$ from the variable coefficient problem for general x). Analogously, $\mathscr{U}^-$ is defined to be the subspace of solutions φ of (2.5) whose corresponding vectors Φ approach, in angle, the subspace $\bar{\mathscr{U}}^-$ as $x \to -\infty$. The existence of these subspaces is established in [GZ] or [K.1, K.2, K.3].

The existence of these subspaces, along with analytic dependence on λ, follows by the gap lemma of [GZ,KS], or alternatively by earlier results of [J,K.1–3]; the full generality of the gap lemma is not needed here, since we have spectral separation of the subspaces $\overline{\mathscr{S}^+}$, $\overline{\mathscr{U}^-}$ and the complementary $\mathbb{A}_\pm$-invariant subspaces, a helpful feature of the scalar case. The necessary hypotheses follow by analytic dependence of $\overline{S^+}$, $\overline{U^-}$, the aforementioned spectral gap, and exponential convergence of the coefficients a, b, and c as $x \to \pm\infty$. Regarding the latter property, recall from Remark 1 that $u_\pm$ are hyperbolic rest points of (2.5) by virtue of (H_2), hence

$$|(d/dx)^\ell(\bar{u} - u_\pm)| \leqslant Ce^{-\alpha|x|}, \quad x \lesseqgtr 0, \quad \ell = 0, 1, 2 \tag{2.14}$$

for some $\alpha > 0$, and thus

$$|a - a_\pm|, |b - b_\pm|, |c - c_\pm| \leqslant Ce^{-\alpha|x|}, \quad x \lesseqgtr 0. \tag{2.15}$$

Using a slight extension of these results (see [ZH] Lemma 3.1, p. 779, or [GZ] Corollary 2.4, p. 807), we can conclude in addition that there exist basis functions $\varphi_j^\pm(\lambda, x)$ such that

$$\mathscr{S}^+ = \mathrm{span}\{\varphi_1^+, \varphi_2^+\}, \tag{2.16}$$

$$\mathscr{U}^- = \mathrm{span}\{\varphi_3^-, \varphi_4^-\}, \tag{2.17}$$

which additionally have symmetry $\varphi_j^\pm(\bar{\lambda}) = \overline{\varphi_j^\pm(\lambda)}$ so that $\varphi_j^\pm$ are real-valued for λ real. This follows from the properties noted above, plus the existence of corresponding basis vectors $V_j^\pm$ asserted in Corollary 2.2. Moreover, the basis functions $\varphi_j^\pm(\lambda, x)$ are analytic in λ at $\lambda = 0$ and continuous elsewhere; the exterior products $\varphi_1^+ \wedge \varphi_2^+$ and $\varphi_3^- \wedge \varphi_4^-$ are analytic on all of $\{\mathrm{Re}\,\lambda \geqslant 0\}$; and $\varphi(\bar{\lambda}) = \overline{\varphi(\lambda)}$ (see [GZ]).

Because their associated eigenvalues may coalesce, φ_1^+, φ_2^+ may not be individually

analytically continuable on $\{\mathrm{Re}\,\lambda \geqslant 0\}$; however, they are jointly continuable in the sense that their span, or alternatively their exterior product, *can* be analytically defined.

2.3 The Evans function

We now define the Evans function, following [AGJS, GZ] as the Wronskian of the basis functions $\varphi_1^+, \varphi_2^+, \varphi_3^-, \varphi_4^-$ that characterize solutions decaying at $+\infty$, at $-\infty$, or both.

$$D(\lambda) := \det \begin{pmatrix} \varphi_1^+ & \varphi_2^+ & \varphi_3^- & \varphi_4^- \\ \varphi_1^{+\prime} & & \cdots & \vdots \\ \varphi_1^{+\prime\prime} & & & \vdots \\ \varphi_1^{+\prime\prime\prime} & & \cdots & \varphi_4^{-\prime\prime\prime} \end{pmatrix}, \tag{2.18}$$

evaluated at $x = 0$. Note that the sign of $D(\lambda)$ is independent of the value of x at which the determinant is evaluated.

Properties

(P1) $D(\cdot)$ is analytic on $\{\mathrm{Re}\,\lambda \geqslant 0\}$.
(P2) $D(\cdot)$ is *real* for real λ.
(P3) On $\{\mathrm{Re}\,\lambda \geqslant 0\}/\{0\}$, $D(\lambda) = 0$ if and only if λ is an eigenvalue of L.

Only (P3) requires discussion. This follows from the characterization of eigenfunctions of L as nontrivial solutions of $(L - \lambda)w = 0$ lying in $\mathscr{S}^+ \cap \mathscr{U}^-$, i.e. decaying at both $\pm\infty$. Evidently, vanishing of the Wronskian $D(\cdot)$ is equivalent to nontrivial intersection of $\mathscr{S}^+$ and $\mathscr{U}^-$, by (2.16)–(2.17).

The meaning of the Evans function at $\lambda = 0$ is less immediate, but equally important. Note that $\lambda = 0$ is an eigenvalue, with at least the eigenfunction $\bar{u}_x$, corresponding to translations of $\bar{u}$. Moreover, since $\bar{u}_x$ decays at $\pm\infty$, it lies in both $\mathscr{U}^-$ and $\mathscr{S}^+$, implying $D(0) = 0$. Moreover, this zero of the Evans function does not interfere with either linear or nonlinear stability, as shown in [HZ.2, ZH], a result we alluded to earlier in formulating condition ($\mathscr{D}$), and which we restate here for clarity.

Proposition 2.3 *Linearized stability of* $\bar{u}(\cdot)$ *as a solution of* (2.1) *w is equivalent to the Evans function condition* ($\mathscr{D}$). *Moreover, linearized stability implies nonlinear stability.*

(**Remark** [HZ.2] also concerns more general, dispersive–diffusive equations such as the convex KdV-Burgers equation, or the nonconvex modified KdV-Burgers equation studied by [D, JMS, W].)

Having defined the Evans function, we now begin to investigate whether or not it has a positive zero. To this end, we use the stability index Γ (see (2.6)) which only requires information about $D(\lambda)$ for sufficiently large λ and the leading order behaviour for real

λ near $\lambda = 0$. The small λ behaviour depends crucially on whether the travelling wave is compressive or undercompressive. The stability index will be shown to be a coordinate-independent orientation of the intersection of the stable/unstable manifolds of u_+/u_- in (2.3). The connection to stability is given through

Proposition 2.4 *The parity of the number of zeroes of $D(\cdot)$ in $\{\mathrm{Re}(\lambda) \geqslant 0\}$ is odd (even) according to $\Gamma > (<)0$. In particular, $\Gamma < 0$ implies instability, whereas $\Gamma > 0$ is necessary for stability.*

Proof Using $D(\bar{\lambda}) = \overline{D(\lambda)}$, we have that complex roots of $D(\cdot)$ appear in conjugate pairs. On the other hand, the number of real roots with $\lambda \geqslant 0$ clearly has the parity claimed.[3] The connection to stability follows from Proposition 2.3. □

2.4 The Evans function as $\lambda \to \infty$

Following [GZ], we now evaluate the Evans function in the large $|\lambda|$ regime. Let $\pi : \mathbb{C}^4 \to \mathbb{C}^4$ denote orthogonal projection onto the span of the first two standard basis elements, $e_1 = (1,0,0,0)^t$ and $e_2 = (0,1,0,0)^t$. We have the following analog of Lemma 3.5 in [GZ]:

Lemma 2.5 *The projection π is full rank on the $\mathbb{A}_\pm$-invariant subspaces $\overline{\mathscr{S}}^+$, $\overline{\mathscr{U}}^-$. Equivalently, if $V = (v_1, v_2, v_3, v_4)^t$ and $\tilde{V} = (\tilde{v}_1, \tilde{v}_2, \tilde{v}_3, \tilde{v}_4)^t \in \overline{\mathscr{S}}^+$ (resp. $\overline{\mathscr{U}}^-$) are independent, then* $\det \begin{pmatrix} v_1 & \tilde{v}_1 \\ v_2 & \tilde{v}_2 \end{pmatrix} \neq 0$.

This result holds for all λ.

Proof It is sufficient to treat the case that V, $\tilde{V}$ are eigenvectors of $\mathbb{A}_\pm$. If they are independent genuine eigenvectors, then, by the companion matrix structure of (2.11), we have $V = (1, \mu, \mu^2, \mu^3)$, $\tilde{V} = (1, \tilde{\mu}, \tilde{\mu}^2, \tilde{\mu}^3)$, and $\det \begin{pmatrix} v_1 & \tilde{v}_1 \\ v_2 & \tilde{v}_2 \end{pmatrix} = \tilde{\mu} - \mu \neq 0$.

The other possibility is that $\mu = \tilde{\mu}$ and $V = (1, \mu, \mu^2, \mu^3)^t$, $\tilde{V} = (0, 1, 2\mu, 3\mu^2)^t$ form an eigenvector/generalized eigenvector pair. In this case, $\det \begin{pmatrix} v_1 & \tilde{v}_1 \\ v_2 & \tilde{v}_2 \end{pmatrix} = 1 \neq 0$, also. □

This lemma allows us to express the sign of $D(\lambda)$ for large λ in terms of the projections of the basis vectors of $\overline{\mathscr{S}}^+$, $\overline{\mathscr{U}}^-$ at $\lambda = 0$. To this end, let the basis vectors $V_j^\pm$ $(j = 1, \ldots, 4)$ have components $V_{jk}^\pm$ $(k = 1, \ldots, 4)$.

Proposition 2.6 *For $\lambda > 0$ real, sufficiently large,*

$$\mathrm{sgn}\ D(\lambda) = \mathrm{sgn}\ \det \begin{pmatrix} V_{11}^+ & V_{21}^+ \\ V_{12}^+ & V_{22}^+ \end{pmatrix} \det \begin{pmatrix} V_{31}^- & V_{41}^- \\ V_{32}^- & V_{42}^- \end{pmatrix} |_{\lambda=0}. \tag{2.19}$$

[3] For example, if $D'(0) > 0$ and $D(\infty) < 0$, then $\Gamma < 0$, and the graph of $D(\lambda)$ over the positive λ axis $0 < \lambda < \infty$ crosses the axis an odd number of times, counting multiplicity. The number of zeroes in the proposition is then even, since the count includes $\lambda = 0$.

Proof The proof follows arguments of Proposition 2.8 of [GZ], or the equivalent Proposition 7.3 of [ZH] for lower order systems of equations. The idea is to use an asymptotic argument for large λ to show that the sign of the determinant in the Evans function can be expressed in terms of the sign of the determinants in (2.19) provided λ is sufficiently large. Then Lemma 2.5, which implies that the sign of the determinants in (2.19) are independent of λ (since they are continuous and can never vanish) gives the desired result.

First we choose λ sufficiently large so that the asymptotic arguments below are valid. We can rescale (2.5) by $\hat{x} = \lambda^{1/4}x$, $\hat{w}(\hat{x}) = w(x)$, $\hat{a}(\hat{x}) = a(x)$, $\hat{b}(\hat{x}) = b(x)$, $\hat{c}(\hat{x}) = c(x)$, to obtain

$$\hat{w}'''' = -\hat{c}^{-1}w + \mathcal{O}(|\lambda^{-1/4}|(|w| + |w'| + |w''| + |w'''|)) \tag{2.20}$$

where $|\hat{c}'| = \mathcal{O}(\lambda^{-1/4})$. Applying Proposition 2.8 of [GZ], or the equivalent Proposition 7.3 of [ZH], we find that in phase variables, the subspaces $\hat{\mathscr{S}}^+(x)/\hat{\mathscr{U}}^-(x)$, defined by the evaluation of the stable/unstable subspace of (2.20) at an arbitrary x_0, lies within angle $\mathcal{O}(\lambda^{-1/4})$ of the stable/unstable subspaces of the limiting equations

$$\hat{w}'''' = -\hat{c}^{-1}w, \tag{2.21}$$

with coefficient $\hat{c}$ held frozen at value $\hat{c}(x_0)$. The subspaces of the limiting equations are spanned by the stable/unstable normal modes of (2.21), readily calculated to be $(1, \hat{\mu}, \hat{\mu}^2, \hat{\mu}^3)^t$, where

$$\hat{\mu} = \hat{\mu}_j(\hat{x}_0) = (-\hat{c}(\hat{x}_0)^{-1})^{1/4} \tag{2.22}$$

are fourth roots of $(-\hat{c})^{-1}$.

Converting back to the original scaling, the subspaces $\mathscr{S}^+(x_0)/\mathscr{U}^-(x_0)$ defined by the evaluation of the stable/unstable subspace of (2.5) at x_0, lie within angle $\mathcal{O}(\lambda^{-1/4})$ of the subspaces spanned by $\{(1, \mu_1, \mu_1^2, \mu_1^3)^t, (1, \mu_2, \cdots, \mu_2^3)^t\}$ and $\{(1, \mu_3, \mu_3^2, \mu_3^3), (1, \mu_4, \mu_4^2, \mu_4^3)\}$ respectively, where

$$\mu_j(x_0) = (-\lambda/c(x_0))^{1/4}. \tag{2.23}$$

Recalling (see § 2.2) that $\mathscr{S}^+(x_0)/\mathscr{U}^-(x_0)$ are real-valued for λ real, and that for large λ μ_1, μ_2 and μ_3, μ_4 form complex conjugate pairs, we find therefore that

$$\begin{pmatrix} \varphi_1^+ & \varphi_2^+ & \varphi_3^- & \varphi_4^- \\ \varphi_1^{+\prime} & \varphi_2^{+\prime} & \varphi_3^{-\prime} & \varphi_4^{-\prime} \\ \varphi_1^{+\prime\prime} & \varphi_2^{+\prime\prime} & \varphi_3^{-\prime\prime} & \varphi_4^{-\prime\prime} \\ \varphi_1^{+\prime\prime\prime} & \varphi_2^{+\prime\prime\prime} & \varphi_3^{-\prime\prime\prime} & \varphi_4^{-\prime\prime\prime} \end{pmatrix} = (1 + \mathcal{O}(|\lambda^{-1/4}|))$$
$$\times \begin{pmatrix} 1 & 1 & 1 & 1 \\ \mu_1 & \mu_2 & \mu_3 & \mu_4 \\ \mu_1^2 & & & \vdots \\ \mu_1^3 & \cdots & & \mu_4^3 \end{pmatrix} \begin{pmatrix} 1/2 & i/2 & 0 & 0 \\ 1/2 & -i/2 & 0 & 0 \\ 0 & 0 & 1/2 & i/2 \\ 0 & 0 & 1/2 & -i/2 \end{pmatrix} \begin{pmatrix} M_+ & 0 \\ 0 & M_- \end{pmatrix} (x_0) \tag{2.24}$$

where $M_{\pm}(x)$ are specific nonsingular real-valued coefficient matrices. It follows, therefore, that

$$D(\lambda) = -(1 + \mathcal{O}(|\lambda^{-1/4}|)) \det \begin{pmatrix} 1 & 1 & 1 & 1 \\ \mu_1 & \mu_2 & \mu_3 & \mu_4 \\ & & & \\ \mu_1^2 & & & \vdots \\ \mu_1^3 & \cdots & & \mu_4^3 \end{pmatrix}_{|x=x_0} \det \begin{pmatrix} M_+ & 0 \\ 0 & M_- \end{pmatrix}. \tag{2.25}$$

Evaluating the Vandermonde determinant, and noting that all quantities involved are real and nonvanishing, hence have sign independent of x_0, we find that

$$\begin{aligned} \operatorname{sgn} D(\lambda) = & \operatorname{sgn} \det i \begin{pmatrix} 1 & 1 \\ \mu_1 & \mu_2 \end{pmatrix} \det M_+|_{x=x_0} \det \begin{pmatrix} 1 & 1 \\ \mu_3 & \mu_4 \end{pmatrix} \det M_-|_{x=x_0} \\ = & \operatorname{sgn} \det i \begin{pmatrix} 1 & 1 \\ \mu_1 & \mu_2 \end{pmatrix} \det M_+|_{x=+\infty} \det \begin{pmatrix} 1 & 1 \\ \mu_3 & \mu_4 \end{pmatrix} \det M_-|_{x=-\infty} \\ = & \operatorname{sgn} \det \begin{pmatrix} V_{11}^+ & V_{21}^+ \\ V_{12}^+ & V_{22}^+ \end{pmatrix} \det \begin{pmatrix} V_{31}^- & V_{41}^- \\ V_{31}^- & V_{42}^- \end{pmatrix} (\lambda) \end{aligned} \tag{2.26}$$

so long as λ is real and sufficiently large.

But, the right hand side of (2.26) is independent of λ by Lemma 2.5. □

Remark 1 The matrices $M_{\pm}$ in the proof are used only as an intermediate book-keeping device, and play no role in the final computation.

2.5 Evaluation at $\lambda = 0$ in the Lax case

In this subsection, we restrict to the *Lax case*, for which

$$a_- > 0 > a_+. \tag{2.27}$$

Consulting Lemma 2.1 and § 2.2, we find that $\mathscr{S}^+(0)$, $\mathscr{U}^-(0)$ consist of all solutions of (2.5) that exponentially decay as $x \to +\infty$, $-\infty$ respectively. We can therefore integrate (2.5) with $\lambda = 0$ from either $+\infty$ or $-\infty$ to obtain

$$c\varphi''' = b\varphi' - a\varphi. \tag{2.28}$$

Note that (2.28) is exactly the *variational equation* for the travelling wave ODE (2.3). Indeed, one solution of (2.28) is $\varphi = \bar{u}_x$, corresponding to translation along the profile. By appropriate change of basis, we can arrange without loss of generality that

$$\varphi_1^+(0, x) = \varphi_4^-(0, x) = \bar{u}'(x). \tag{2.29}$$

We choose φ_2^+ and φ_3^- to be any independent solutions of (2.28) decaying at $\pm\infty$.

Note that the travelling wave ODE (2.3) can be written as a three dimensional autonomous system

$$\begin{aligned} u' &= u_1, \\ u_1' &= u_2, \\ u_2' &= \frac{b(u)}{c(u)} u_1 - \frac{f(u) - f(u_-)}{c(u)}, \end{aligned} \tag{2.30}$$

which has equilibria at $B = (u_+, 0, 0)$ and $M = (u_-, 0, 0)$. A travelling wave solution of (2.3) connecting u_- to u_+ corresponds to a heteroclinic orbit of (2.30) connecting M to B. For the Lax case, M has a two-dimensional unstable manifold and B has a two-dimensional stable manifold. We now see that the subspace $\mathscr{S}^+$ ($\mathscr{U}^-$) at $\lambda = 0$ is composed of functions φ with corresponding vectors $(\varphi, \varphi', \varphi'')^t$ that span the tangent space of $W^s(B)$ ($W^u(M)$) along $\bar{u}(\cdot)$. An illustration of this structure for the special case of (1.6) is presented at the end of this section.

The next proposition, following the general approach introduced by Jones [J] relates the sign of $D'(0)$ to the orientation with which these stable/unstable manifolds intersect in the phase space $\mathbb{R}^3$ of (2.3).

Proposition 2.7 *$D(0) = 0$, while*

$$\operatorname{sgn} D'(0) = \operatorname{sgn} c(0)^{-1} \det \begin{pmatrix} \bar{u}_x & \varphi_2^+ & \varphi_3^- \\ \bar{u}_x' & \varphi_2^{+'} & \varphi_3^{-'} \\ \bar{u}_x'' & \varphi_2^{+''} & \varphi_3^{-''} \end{pmatrix} (u_+ - u_-). \tag{2.31}$$

Proof

$$D(0) = \det \begin{pmatrix} \bar{u}_x & \varphi_2^+ & \varphi_3^- & \bar{u}_x \\ \vdots & \vdots & \vdots & \vdots \\ \bar{u}_x''' & (\varphi_2^+)''' & (\varphi_3^-)''' & \bar{u}_x''' \end{pmatrix} = 0. \tag{2.32}$$

Similarly, a straightforward calculation (as in [GZ]) yields

$$D'(0) = \det \begin{pmatrix} \bar{u}_x & \varphi_2^+ & \varphi_3^- & (\varphi_{4_\lambda}^- - \varphi_{1_\lambda}^+) \\ \vdots & \vdots & \vdots & \vdots \\ \bar{u}_x''' & \varphi_2^{+'''} & \varphi_3^{-'''} & (\varphi_{4_\lambda}^- - \varphi_{1_\lambda}^+)''' \end{pmatrix}. \tag{2.33}$$

Differentiation of (2.5) with respect to λ shows that the functions $z = \varphi_{1_\lambda}^+$, $\varphi_{4_\lambda}^-$ satisfy the same variational equation

$$(cz''')' = (bz')' - (az)' - \bar{u}_x, \tag{2.34}$$

decaying at $+\infty$, $-\infty$ respectively. Integrating from $+\infty$, $-\infty$ respectively, and subtracting, we find that $\tilde{z} := \varphi_{4_\lambda}^- - \varphi_{1_\lambda}^+$ satisfies

$$c\tilde{z}''' = b\tilde{z}' - a\tilde{z} + (u_- - u_+), \tag{2.35}$$

an inhomogeneous version of (2.28). Using (2.28), (2.35) to eliminate the fourth row in (2.33), we obtain

$$D'(0) = c(0)^{-1} \det \begin{pmatrix} \bar{u}_x & \varphi_2^+ & \varphi_3^- & \tilde{z} \\ \bar{u}_x' & \varphi_2^{+'} & \varphi_3^{-'} & \tilde{z}' \\ \bar{u}_x'' & \varphi_2^{+''} & \varphi_3^{-''} & \tilde{z}'' \\ 0 & 0 & 0 & (u_- - u_+) \end{pmatrix}, \tag{2.36}$$

giving the result. □

Remark The right-hand side of (2.36) is of the form $\gamma\Delta$, where the first factor, γ measures orientation of the intersection of the stable and unstable manifolds of the underlying

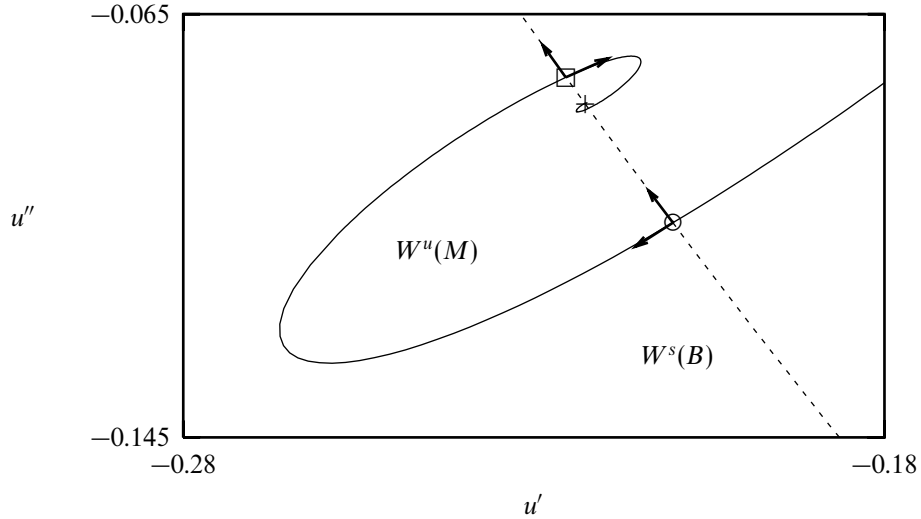

FIGURE 4. Section of the invariant manifolds $W^u(M)$ (solid line), $W^s(B)$ (dashed line) and $W^u(T)$ (plus) with the Poincaré plane $P = \{(u, u', u''); u = (2u_- + u_+)/3\}$. Intersections of the solid and dashed lines mark points where trajectories connecting M to B hit P. The symbols around these intersections indicate whether the corresponding profile is a stable (circles) or unstable (boxes) solution of the PDE, for the first two travelling waves $\bar{u}$. Arrows indicate the direction of $((\varphi_2^+), (\varphi_2^+)')$ and $((\varphi_3^-), (\varphi_3^-)')$ (the projection of the derivative vectors on the Poincaré plane).

travelling wave ODE at u_+, u_- respectively, and the second factor, $\Delta = [u]$, is the Kreiss–Sakamoto–Lopatinski determinant arising in the study of inviscid stability. This is a special case of a very general relation pointed out in [ZS] between viscous and inviscid stability.

Combining Propositions 2.6 and 2.7, we have

Corollary 2.8 *The stability index* $\Gamma := \operatorname{sgn} D'(0)D(+\infty)$ *satisfies*

$$\Gamma = \operatorname{sgn}\left[\begin{pmatrix} \bar{u}_x & \varphi_2^+ & \varphi_3^- \\ \bar{u}_x' & \varphi_2^{+\prime} & \varphi_3^{-\prime} \\ \bar{u}_x'' & \varphi_2^{+\prime\prime} & \varphi_3^{-\prime\prime} \end{pmatrix}|_{x=0} \times \det\begin{pmatrix} \bar{u}_x & \varphi_2^+ \\ \bar{u}_x' & \varphi_2^{+\prime} \end{pmatrix}|_{x=+\infty} \det\begin{pmatrix} \varphi_3^- & \bar{u}_x \\ \varphi_3^{-\prime} & \bar{u}_x' \end{pmatrix}|_{x=-\infty}(u_- - u_+)\right].$$

We now present an example from [BMS99] and discuss how the machinery developed here explains numerical observations of one dimensional stability of compressive waves. We consider (1.6) with $\beta = 0$ and $\gamma = 1$. For each u_+ there is a range of u_- for which multiple compressive travelling waves appear. For a special value of u_- an infinite number of compressive waves occur. For the case $u_+ = 0.1$, the special value is approximately $u_- = 0.332051$. A detailed discussion of the phase portrait for this example is given in [BMS99]. Shown in Figure 4 is a Poincaré section (at fixed u) from the phase portrait of (2.30). The stable manifold $W^s(B)$ is shown as a dashed line while the unstable manifold

$W^u(M)$ is shown as a solid line. Note that this unstable manifold appears as a spiral whose center corresponds to the undercompressive connection. Each intersection of these two curves denotes a point along a heteroclinic orbit of (2.30). The intersection denoted by a circle corresponds to a one-dimensionally stable compressive wave while the box corresponds to a one dimensionally unstable compressive wave. The arrows on the figure denote the orientation of a choice of basis vectors $((\varphi_2^+),(\varphi_2^+)')$ and $((\varphi_3^-),(\varphi_3^-)')$. Note that the orientation of these vectors switches at each successive crossing of the spiral. The vector $(\bar{u}_x, \bar{u}_x', \bar{u}_x'')$ is into the Poincaré plane. Following Corollary 2.8, the corresponding stability indices Γ_j *alternate in sign*. This is consistent with numerical observations that the successive waves alternate stability. (Recall that $u_\pm$ are fixed. The remaining terms $\det \begin{pmatrix} \bar{u}_x & \varphi_2^+ \\ \bar{u}_x' & \varphi_2^{+\prime} \end{pmatrix}$ and $\det \begin{pmatrix} \varphi_3^- & \bar{u}_x \\ \varphi_3^{-\prime} & \bar{u}_x' \end{pmatrix}$ fix a common orientation on the stable/unstable manifolds at u_-/u_+).

Remark As often happens, we obtain a rigorous *instability* result by this technique, but it is only suggestive of stability. To obtain a complete stability result would require establishing nonexistence of pure imaginary eigenvalues (other than $\lambda = 0$), a separate (and quite interesting) unresolved issue.

2.6 Evaluation at $\lambda = 0$ in the undercompressive case

The undercompressive case, $\operatorname{sgn} a_- = \operatorname{sgn} a_+$, can be treated similarly. For example, Proposition 2.6 goes through unchanged. However, the behaviour at $\lambda = 0$ is significantly different, as might be expected from the fact that long-wave behaviour is dominated by the convection rates $a_\pm$ in the far field. In the present, one-dimensional context, this leads to a slightly modified stability index. In the context of multi-dimensional stability, as we shall see later, the distinction is still more critical.

Without loss of generality (and to be consistent with the thin film context [BMS99]), assume

$$a_- = f'(u_-), a_+ = f'(u_+) < 0. \tag{2.37}$$

Note that this implies that there exists an intermediate equilibrium[4] u_m between u_- and u_+. The corresponding system of equations (2.30) describing the phase portrait for the travelling wave has (at least) three equilibria $B = (u_+, 0, 0)$, $M = (u_m, 0, 0)$, $T = (u_-, 0, 0)$. The undercompressive wave corresponds to a connection from T (which has a one-dimensional unstable manifold) to B (with a two-dimensional stable manifold).

Appealing again to § 2.2, we find that, as in the Lax case, $\mathscr{S}^+$ consists of all solutions of (2.5) decaying exponentially at $x = +\infty$. However, recalling the discussion before Corollary 2.2, when $\lambda = 0$, $\mathscr{U}^-$ now consists of solutions that are only *bounded* as $x \to -\infty$. Without loss of generality, when $\lambda = 0$, choose again $\varphi_1^+(x) = \varphi_4^-(x) = \bar{u}_x(x)$, and take φ_2^+, φ_3^- to be independent solutions of (2.5) in $\mathscr{S}^+$, $\mathscr{U}^-$ respectively, where we can choose the normalization $\varphi_3^-(-\infty) = 1$.

[4] Note that we are using slightly different notation from [BMS99] in which u_- and u_+ always denote nearest equilibria.

Proposition 2.9 *$D(0) = 0$, while*

$$\begin{aligned} \operatorname{sgn} D'(0) &= -\operatorname{sgn}(a_-/c(0)) \det \begin{pmatrix} \bar{u}_x & \varphi_2^+ & (z^- - z^+) \\ \bar{u}_x' & \varphi_2^{+\prime} & (z^- - z^+)' \\ \bar{u}_x'' & \varphi_2^{+\prime\prime} & (z^- - z^+)'' \end{pmatrix} |_{x=0} \\ &= \operatorname{sgn} a_- \int_{-\infty}^{\infty} (1/c)(\bar{u} - u_-) \det \begin{pmatrix} \bar{u}_x & \varphi_2^+ \\ \bar{u}_x' & \varphi_2^{+\prime} \end{pmatrix} dx, \end{aligned} \tag{2.38}$$

where $z^{\pm}$ satisfies the variational equation

$$cz''' = bz' - az - (\bar{u} - u_-), \tag{2.39}$$

with

$$z^+(+\infty) = 0, \qquad z^-(-\infty) = (u_+ - u_-)/a_-. \tag{2.40}$$

Proof As in the proof of Proposition 2.7,

$$D(0) = \det \begin{pmatrix} \bar{u}_x & \varphi_2^+ & \varphi_3^- & \bar{u}_x \\ \vdots & \vdots & \vdots & \vdots \\ \bar{u}_x''' & (\varphi_2^+)''' & (\varphi_3^-)''' & \bar{u}_x''' \end{pmatrix} = 0, \tag{2.41}$$

and

$$D'(0) = \det \begin{pmatrix} \bar{u}_x & \varphi_2^+ & \varphi_3^- & (\varphi_{4_\lambda}^- - \varphi_{1_\lambda}^+) \\ \vdots & \vdots & \vdots & \vdots \\ \bar{u}_x''' & \varphi_2^{+\prime\prime\prime} & \varphi_3^{-\prime\prime\prime} & (\varphi_{4_\lambda}^- - \varphi_{1_\lambda}^+)''' \end{pmatrix}. \tag{2.42}$$

Likewise, the **decaying solutions** $\bar{u}_x$ and φ_2^+ satisfy equation (2.28). However, φ_3^- is asymptotically constant, $\varphi_3^-(-\infty) = 1$, hence satisfies the inhomogeneous equation

$$c\varphi''' = b\varphi' - a\varphi + a_-. \tag{2.43}$$

Using the fact that $\tilde{z} := \varphi_{4_\lambda}^- - \varphi_{1_\lambda}^+$ as before satisfies (2.35), we can use (2.28), (2.35), (2.43) to reduce the fourth row of (2.42), obtaining

$$D'(0) = c^{-1} \det \begin{pmatrix} \bar{u}_x & \varphi_2^+ & \varphi_3^- & \tilde{z} \\ \bar{u}_x' & \varphi_2^{+\prime} & \varphi_3^{-\prime} & \tilde{z}' \\ \bar{u}_x'' & \varphi_2^{+\prime\prime} & \varphi_3^{-\prime\prime} & \tilde{z}'' \\ 0 & 0 & a_- & u_- - u_+ \end{pmatrix}. \tag{2.44}$$

Using the third column to eliminate $(u_+ - u_-)$, we obtain

$$D'(0) = c^{-1} \det \begin{pmatrix} \bar{u}_x & \varphi_2^+ & \varphi_3^- & z^- - z^+ \\ \bar{u}_x' & \varphi_2^{+\prime} & \varphi_3^{-\prime} & (z^- - z^+)' \\ \bar{u}_x'' & \varphi_2^{+\prime\prime} & \varphi_3^{-\prime\prime} & (z^- - z^+)'' \\ 0 & 0 & a_- & 0 \end{pmatrix}, \tag{2.45}$$

where $z^- - z^+ = \tilde{z} - \left(\frac{u_- - u_+}{a_-}\right) \varphi_3^-$ are defined by

$$z^+ := \varphi_{1_\lambda}^+, \qquad z^- := \varphi_{4_\lambda}^- - \left(\frac{u_- - u_+}{a_-}\right) \varphi_3^-. \tag{2.46}$$

Evaluation of (2.45) at $x = 0$ gives the first equality in (2.38). Integration of (2.34), together

with (2.43), verify that $z^{\pm}$ both satisfy (2.39), with the claimed boundary conditions at $\pm\infty$.

Now define

$$\Psi^{\pm} := \det \begin{pmatrix} \bar{u}_x & \varphi_2^+ & z^{\pm} \\ \bar{u}_x' & \varphi_2^{+'} & z^{\pm'} \\ \bar{u}_x'' & \varphi_2^{+''} & z^{\pm''} \end{pmatrix}. \tag{2.47}$$

The reduction to a *Melnikov integral* in the second equality in (2.38) involves evaluation of $\Psi^- - \Psi^+$. Briefly, this follows (e.g. see, [GZ], proof of Lemma 3.4, or [GH, Sch]) from the (inhomogeneous) Abel's formula,

$$\begin{aligned} \psi' &= Tr\mathbb{B}\,\psi + \det \begin{pmatrix} \bar{u}_x & \varphi_2^+ & 0 \\ \vdots & \vdots & 0 \\ \bar{u}_x'' & \varphi_2^{+''} & (\bar{u}-u_-) \end{pmatrix} \\ &= \det \begin{pmatrix} \bar{u}_x & \varphi_2^+ & 0 \\ \vdots & \vdots & 0 \\ \bar{u}_x'' & \varphi_2^{+''} & (\bar{u}-u_-) \end{pmatrix}, \end{aligned} \tag{2.48}$$

and Duhamel's principle/variation of constants, to evaluate $\Psi^{\pm}$ at $x = 0$. Here,

$$\mathbb{B} = \mathbb{B}(\lambda, x) \begin{pmatrix} 0 & 1 & 0 \\ 0 & 0 & 1 \\ -a/c & b/c & 0 \end{pmatrix}$$

denotes the coefficient matrix for (2.28) written as a first order system. □

Combining Corollary 2.8 and Proposition 2.9, and recalling that, as $x \to -\infty$, $(\phi_3^-, \phi_3^{-\prime}) \to (1,0)$ and $\operatorname{sgn} \bar{u}_{xx} \sim \operatorname{sgn} \mu_4^- \bar{u}_x = \operatorname{sgn} \bar{u}_x$, we have

Corollary 2.10 *The stability index* $\Gamma := \operatorname{sgn} D'(0)D(+\infty)$ *is given by*

$$\Gamma = \operatorname{sgn} a_- \int_{-\infty}^{\infty} (1/c)(\bar{u}-u_-) \det \begin{pmatrix} \bar{u}_x & \varphi_2^+ \\ \bar{u}_x' & \varphi_2^{+'} \end{pmatrix} dx\ \bar{u}_x(-\infty) \det \begin{pmatrix} \bar{u}_x & \varphi_2^+ \\ \bar{u}_x' & \varphi_2^{+'} \end{pmatrix} |_{x=+\infty} \tag{2.49}$$

Note that the functions $z^{\pm}$ in (2.38) are uniquely specified by (2.39)–(2.40), modulo $\operatorname{span}\{\bar{u}_x, \varphi_2^+\}$. z^- and z^+ have an important interpretation as the variations, in the travelling wave ODE,

$$c(u)u''' = b(u)u' - (f(u) - f(u_-) - s(u-u_-)), \tag{2.50}$$

of the unstable/stable manifolds of u_+ and $u_-(s)$ as the shock speed s is varied. Likewise,

$$\frac{1}{c(0)} \det \begin{pmatrix} \bar{u}_x & \varphi_2^+ & (z^- - z^+) \\ \vdots & \vdots & \vdots \\ \bar{u}_x'' & \varphi_2^{+''} & (z^- - z^+)'' \end{pmatrix} |_{x=0} = \int_{-\infty}^{\infty} (1/c)(\bar{u}-u_-) \det \begin{pmatrix} \bar{u}_x & \varphi_2^+ \\ \bar{u}_x' & \varphi_2^{+'} \end{pmatrix} \tag{2.51}$$

can be recognized as $\frac{\partial d}{\partial s}|_{s=0}$, where $d(s)$ is the *Melnikov separation function*, measuring the distance (in three-dimensional phase space) between the one dimensional unstable manifold T and the two dimensional stable manifold of B along a fixed transverse section. Alternatively, it represents the orientation with which $\mathscr{S}^+$ and $\mathscr{U}^-$ intersect in

four-dimensional phase space of equation (2.50) augmented with

$$s' = 0. \tag{2.52}$$

The stability index Γ is a coordinate- and normalization-independent measure of the orientation.

Calculation of Γ We now turn to the calculation of the stability index for the undercompressive case, which hinges on the calculation of the sign of the Melnikov integral

$$\partial d/\partial s = \int_{-\infty}^{\infty} (1/c)(\bar{u} - u_-) \det \begin{pmatrix} \bar{u}_x & \varphi_2^+ \\ \bar{u}_x' & \varphi_2^{+\prime} \end{pmatrix} dx.$$

This can be evaluated conveniently in terms of the left zero eigenfunction π^0. We postpone a discussion of the associated spectral theory to the next section. It transpires that the Melnikov integral arising in calculation of the stability index for undercompressive shocks can be expressed alternatively as

$$\langle \bar{u} - u_*, k\pi_x^0 \rangle, = \langle \bar{u}_x, k\pi^0 \rangle = k, \tag{2.53}$$

where $\langle \cdot, \cdot \rangle$ denotes L^2 inner product, u_* is the state arising in the original formula (in the present setting, $u_* = u_-$; see [GZ] for more general situations), and k is an appropriately chosen constant. The key simplification of the Melnikov integral comes from the formula

$$k\pi_x^0 = (1/c) \det \begin{pmatrix} \bar{u}_x & \varphi_2^+ \\ \bar{u}_x' & \varphi_2^{+\prime} \end{pmatrix}, \tag{2.54}$$

which we derive below. Comparing behaviours at $+\infty$, we find that the sign of the Melnikov integral is

$$\text{sgn } (1/c) \det \begin{pmatrix} \bar{u}_x & \phi_2^+ \\ \bar{u}_x' & \phi_2^{+\prime} \end{pmatrix} \pi_x^0|_{x=+\infty},$$

and thus, referring back to (2.49), we obtain the simple expression:

Proposition 2.11 *For an undercompressive wave, the stability index Γ can be computed as*

$$\Gamma = \text{ sgn } a_- \pi_x^0(+\infty)\bar{u}_x(-\infty) \tag{2.55}$$

where π^0 denotes the left zero eigenfunction.

For the specific travelling wave computed numerically and shown in Figure 5 and for the corresponding π^0 shown in Figure 7, we observe that $\Gamma = +1$, consistent with the stability of the undercompressive wave. To finish the proof of Proposition 2.11 we show the equality (2.54) then use integration by parts and the fact that $\pi^0(+\infty) = 0$. As we discuss in more detail in the next section, π^0 is uniquely specified up to a constant factor, is bounded, and satisfies the adjoint eigenvalue equation

$$-(cz')''' + (bz')' + az' = 0.$$

It follows that the derivative π_x^0 is uniquely specified up to constant factor by the properties that it decays at $\pm\infty$ and satisfies

$$-cy''' + (by)' + ay = 0, \tag{2.56}$$

obtained by setting $y = z'$.

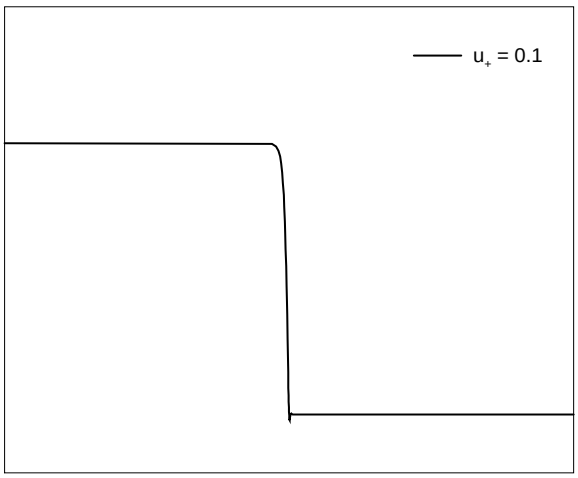

FIGURE 5. The undercompressive wave corresponding to $\beta = 0$, $\gamma = 1$, and $u_+ = 0.1$.

Now, observe that, by Abel's formula, the vector (e_1, e_2, e_3) defined by

$$e_1 = \det \begin{pmatrix} \bar{u}_x' & \varphi_2^{+\prime} \\ \bar{u}_x'' & \varphi_2^{+\prime\prime} \end{pmatrix},$$

$$e_2 = -\det \begin{pmatrix} \bar{u}_x & \varphi_2^{+} \\ \bar{u}_x' & \varphi_2^{+\prime\prime} \end{pmatrix},$$

and

$$e_3 = \det \begin{pmatrix} \bar{u}_x & \varphi_2^{+} \\ \bar{u}_x' & \varphi_2^{+\prime} \end{pmatrix},$$

must satisfy $e_1 w + e_2 w' + e_3 w'' \equiv \textit{constant}$ for any solution w of the linearized travelling wave equation

$$-cw''' + bw' - aw = 0,$$

of which both $\bar{u}_x$ and ϕ_2^+ are solutions.

It follows that (e_1, e_2, e_3) must satisfy the adjoint ODE to the linearized travelling wave equation written as first order system $W' = \mathscr{B}^t W$, where $\mathscr{B}$ is as in (2.6),

$$\mathscr{B}^t = \begin{pmatrix} 0 & 0 & a/c \\ -1 & 0 & -b/c \\ 0 & -1 & 0 \end{pmatrix},$$

from which we readily find that e_3 satisfies

$$e_3''' - (be_3/c)' - (a/c)e_3 = 0.$$

Thus,

$$(1/c)\det \begin{pmatrix} \bar{u}_x & \varphi_2^{+} \\ \bar{u}_x' & \varphi_2^{+\prime} \end{pmatrix} = (1/c)e_3$$

satisfies (2.56) as claimed.

Remarks The formula (2.55) in Proposition 2.11 is new, and is not restricted to the special setting of thin film models. In fact, the ideas used in its derivation, in particular (2.53) and (2.54), easily generalize to systems of conservation laws of arbitrary order to yield an analogous result. These formulae are the consequence of a general but somewhat nonstandard duality principle.[5]

This observation therefore represents a useful refinement in the general theory. For comparison, the formulae obtained in [GZ] for second order diffusive systems is analogous to Corollary 2.10; in the third order scalar case treated in [D] the formula obtained are explicitly evaluable, and the issue does not arise.

As pointed out in [SSch] in the diffusive case, nonvanishing of the Melnikov integral is related to well-posedness of Riemann solutions near the undercompressive shock (u_-, u_+, s). There is, however, no analog of (2.31) in the diffusive case, for which scalar Lax shocks are always stable [S.1, H.1, H.2, H.3, JGK].

In both the Lax and undercompressive cases, the index Γ can be evaluated numerically. However, it does not give a conclusive result of stability, yielding only parity of the number of unstable eigenvalues of L.

A complete numerical evaluation of stability can be performed efficiently using an algorithm of Brin [Br], in which $D(\cdot)$ itself is evaluated numerically, and the winding number computed around $\{\mathrm{Re}\,\lambda \geqslant 0\}$. Moreover, the largest eigenvalue can be computed numerically using the power method discussed in the following section. Furthermore, as was done in [BMS99], nonlinear stability can be verified numerically by perturbing the stationary wave and noting convergence or divergence of solutions of the PDE.

[5] In particular, note that the fact that e_3/c satisfies the equation for z' can be seen from the more general relation

$$(z', z'', z''')\tilde{\mathscr{S}}(w, w', w'')^t \equiv constant$$

for solutions w of the linearized travelling wave ODE (in particular, decaying solutions of the adjoint ODE at $\lambda = 0$) and solutions z of the adjoint eigenvalue ODE at $\lambda = 0$, where

$$\tilde{\mathscr{S}} := \begin{pmatrix} -b + c'' & -c' & c \\ 2c' & -c & 0 \\ c & 0 & 0 \end{pmatrix}. \tag{N1}$$

For, by duality, this implies that $(z', z'', z''')\tilde{\mathscr{S}} =: (e_1, e_2, e_3)$, solves the adjoint of the travelling wave ODE written as a first order system, and by inspection $e_3 = cz'$.

This relation, in turn, is a special case of

$$(z, z', z'', z''')\mathscr{S}(w, w', w'', w''')^t \equiv constant$$

for solutions w, z of the eigenvalue and (resp.) adjoint eigenvalue ODE at $\lambda = 0$, where

$$\mathscr{S} := \begin{pmatrix} a & b + c'' & -c' & c \\ -b - c'' & 2c' & c & 0 \\ -c' & -c & 0 & 0 \end{pmatrix}, \tag{N2}$$

under assumption $cw''' = bw' - aw$. The duality relation (N1) was pointed out in [LZ.2] in the second-order diffusive (system) case; the underlying relation (N2) was pointed out in [ZH], Lemma 4.4, and the extension to arbitrary higher order operators discussed in [ZH], proof of Theorem 6.3.

3 Multi-dimensional stability and the long-wave paradox

This section addresses multi-dimensional stability and the long-wave paradox for stability of undercompressive shocks. Here we are concerned with how the spectrum of the linearized operator depends upon the transverse wave number. For this problem, we present a theoretical justification for formal and numerical treatments of the spectral problem.

A first order perturbation analysis of the spectrum can be readily carried out, both for systems and for scalar equations, by Evans function calculations very similar to those of the previous section [ZS]. What we require here, however, is a *second order* expansion, or 'diffusive correction' in the language of [ZS], since scalar shock fronts are always neutrally stable to first order (see [ZS], or calculations just below). In the present, scalar setting, this is much more convenient to carry out via standard, Fredholm solvability calculations, justified by passing to an appropriate weighted norm, than via the Evans function framework, and we shall therefore take this different point of view in what follows.

3.1 Preliminaries

Consider now the multi-dimensional version

$$u_t + f(u)_x = \nabla \cdot (b(u)\nabla u) - \nabla \cdot (c(u)\nabla \Delta u) \tag{3.1}$$

of equation (2.1). Linearizing about $\overline{u}(\cdot)$, and taking the Fourier transform in transverse directions, we obtain

$$\hat{v}_t = L_k \hat{v} := -(c\hat{v}_{xxx})_x + (b\hat{v}_x)_x - (a\hat{v})_x - k^2(b\hat{v} - (c\hat{v}_x)_x - c\hat{v}_{xx}) - k^4 c\hat{v} \tag{3.2}$$

where

$$c = c(\overline{u}), \quad b = b(\overline{u}), \quad a = f'(\overline{u}) - b'(\overline{u})\overline{u}_x + c'(\overline{u})\overline{u}_{xxx}, \tag{3.3}$$

and k is the wave number, $\hat{v} = \hat{v}(x, k, t)$.

Remark Equation (3.2) is for two space dimensions as in the application to thin films. In the case of higher dimensions, rotational invariance yields the same transformed equation in which k becomes the modulus of the wavenumber.

Associated with (3.2), we have the family

$$(L_k - \lambda I)w = 0 \tag{3.4}$$

of eigenvalue equations, where L_0 is exactly the linearized operator about $\overline{u}(x)$ for the one-dimensional problem. In what follows, we will assume L_k is an analytic function of k^2, rather than just k, since in equation (3.2), L_k is a quadratic polynomial of k^2.

The question, assuming stability of the one-dimensional operator, is whether the spectrum of L_k *remains* stable as k is varied. Of particular interest (e.g. see [CE]) is the variation for small k of the largest eigenvalue $\lambda(k)$, where $\lambda(0) = 0$ corresponds to translation of the wave. For it is this mode, to leading order, that governs the propagation of disturbances along the front [G, GM, HZ.2, K.1, K.2, K.3, KS, ZH, ZS]. Stability of $\lambda(k)$ for small k

(i.e. $\operatorname{Re}\lambda \leqslant 0$) is called *long-wave stability*. This is the problem of most interest since the fourth order diffusion necessarily causes the dominant eigenvalue to decay as $-k^4c$ for large values of $|k|$.

3.2 Spectral Theory

A rigorous discussion of long-wave stability, in the context of conservation laws, requires additional spectral perturbation theory, beyond the usual Banach space theory of, for example, [K, Y]. The eigenvalue $\lambda(0) = 0$ of main interest is embedded in the essential spectrum of L_0, [He, S.1, ZH] hence this standard theory does not apply. *A priori* there is no reason to expect an analytic development of $\lambda(k)$ at such a point; indeed, for systems of conservation laws, it is a fundamental fact that $\lambda(\cdot)$ is in general *not* analytic at $k = 0$. We refer the reader to [ZS] for further discussion of this general situation.

However, in the present, scalar context, a much simpler treatment is possible by the weighted norm method of Sattinger [S.2]. Introducing the norm

$$\|f\|_\Omega := \|f\Omega\|_{L^2}, \tag{3.5}$$

with

$$\Omega(x) := e^{-\theta\int_0^x a(y)dy}, \quad 1 > \theta > 0, \tag{3.6}$$

has the effect of shifting the essential spectrum of L_0 to the left, into the strictly stable complex half-plane, as is readily checked by the methods of [He, S.2] (see also [Z.2] for further details). Thus, in this norm, $\lambda(0) = 0$ becomes an isolated eigenvalue, and we may conclude from standard spectral theory the existence of analytical developments

$$\lambda(k) = \lambda^1 k^2 + \cdots, \tag{3.7}$$

and

$$\varphi(k) = \varphi^0 + \varphi^1 k^2 + \cdots, \tag{3.8}$$

of λ and the associated right eigenfunction $\varphi \in L^2_\Omega$.

Likewise, there exists an analytic L^2_Ω left eigenfunction with respect to the L^2_Ω inner product, whence we can conclude existence of an analytic eigenfunction

$$\pi(k) = \pi^0 + \pi^1 k^2 + \cdots, \tag{3.9}$$

with respect to the standard inner product, where $\Omega^{-2}\pi \in L^2_\Omega$, or equivalently

$$\pi \in L^2_{\Omega^{-1}}. \tag{3.10}$$

Moreover, λ/φ are the unique L^2_Ω eigenvalue/function pair for L_k in the vicinity of $\lambda = 0$, and λ/π the unique $L^2_{\Omega^{-1}}$ pair.

An interesting feature of these developments as compared to the usual (unweighted) type is that, depending on the signs of $a_\pm$, $\varphi(k)$ or $\pi(k)$ may be nondecaying, in fact *exponentially growing* at $\pm\infty$. Nonetheless, as in the classical case, we have the following result, in which $\langle\cdot,\cdot\rangle$ denotes the standard $L^2(\mathbb{R})$ inner product:

Proposition 3.1 *Suppose that (consistent with one-dimensional stability) $\lambda = 0$ is a simple eigenvalue of L_0 (i.e. when $k = 0$), and that all other eigenvalues have a negative real part.*

Let $\lambda(k)$ as above denote the largest eigenvalue of L_k. Then, for compactly supported initial data v_0, and x restricted to any bounded domain, the solution $v(x,t) = e^{L_k t}v_0(x)$ of $v_t = L_k v$ satisfies

$$v(x,t) = e^{\lambda(k)t}\mathscr{P}(k)v_0(1 + \mathcal{O}(e^{-\eta t})), \quad \eta > 0, \tag{3.11}$$

where $\mathscr{P}(k)$ denotes the generalized spectral projection operator

$$\mathscr{P}(k)g := \varphi(k)\langle \pi(k), g\rangle \tag{3.12}$$

associated with $\lambda(k)$.

This can be seen from the corresponding classical result in L^2_Ω, together with the observation that Ω is bounded above and below on compact domains. For a proof in the general, systems setting, see [ZH, sections 5–6 and 8], (note: this result is independent of the regularity of $\lambda(\cdot)$.)

Proposition 3.1 states that the nonstandard eigenfunctions φ, π still govern asymptotic behaviour on bounded domains, analogous to 'resonant poles' in scattering theory [LP]. A useful corollary of this fact is that the *power method* can be used to find the largest eigenvalue/eigenfunction of L_k, by solving $v_t = L_k v$ starting with any compactly supported initial data. This validates the numerical stability analysis of [BB97, BMFC98].

Likewise, the classical formula

$$\lambda^1 = \langle \pi^0, L^1\varphi^0\rangle + \langle \pi^0, (L^0 - \lambda^0)\varphi^1\rangle = \langle \pi^0, L^1\varphi^0\rangle \tag{3.13}$$

($L_k =: L^0 + kL^1 + \cdots$) based on solvability conditions/Fredholm alternative can be seen to apply, as a consequence of the equivalent formula in the Ω norm. That all L^2 inner products are well-defined follows from consideration of the decay/growth of φ, π as $x \to \pm\infty$, which reveals that they and their derivatives lie in L^2_Ω, $L^2_{\Omega^{-1}}$, respectively. (By comparison, only a weak version of the Fredholm alternative survives for systems, see [ZH].)

Remark The introduction of the weighted norm $\|\cdot\|_\Omega$ is equivalent to the change of variables $z = \Omega w$, from which observation we may deduce that (since such a change of variables introduces only a nonzero constant multiplier) that zeroes of the Evans function correspond to eigenvalues with respect to Ω norm. Moreover, this yields the useful characterization of their generalized eigenfunctions as the intersection between the stable/unstable manifolds $\mathscr{S}^+/\mathscr{U}^-$ defined as in § 2.

To investigate long-wave stability, we expand the operator L_k in powers of k^2, $L_k = L^0 + k^2L^1 + k^4L^2$, with

$$L^0 := L_0, \qquad L^1 = -b + \frac{d}{dx}\left(c\frac{d}{dx}\right) + c\frac{d^2}{dx^2}, \qquad L^2 = -c. \tag{3.14}$$

Using the fact that $\varphi^0 = \bar{u}_x$, to first order we obtain

$$\lambda^1\bar{u}_x = L^1\bar{u}_x + L^0\varphi^1.$$

We multiply this equation with the left eigenfunction of L_0, i.e. the solution of

$$L_0^* \pi^0 = 0, \tag{3.15}$$

where

$$L_0^* = -\frac{d^3}{dx^3}\left(c\frac{d}{dx}\right) + \frac{d}{dx}\left(b\frac{d}{dx}\right) + a\frac{d}{dx} \tag{3.16}$$

is the formal adjoint, and then integrate from $-\infty$ to $+\infty$, to get

$$\lambda^1 \int_{-\infty}^{\infty} \pi^0 \bar{u}_x = \int_{-\infty}^{\infty} \pi^0 L^1 \bar{u}_x + \int_{-\infty}^{\infty} \pi^0 L^0 \varphi^1.$$

Integration by parts of the last term yields

$$\int_{-\infty}^{\infty} \pi^0 L^0 \varphi^1 = \int_{-\infty}^{\infty} \varphi^1 L_0^* \pi^0 = 0, \tag{3.17}$$

since the boundary terms vanish.

Hence,

$$\lambda^1 \int_{-\infty}^{\infty} \pi^0 \bar{u}_x = \int_{-\infty}^{\infty} \pi^0 L^1 \bar{u}_x,$$

as in (3.13) if π^0 is normalized by $< \pi^0, \bar{u}_x >= 1$.

Hence, using the explicit expression for L^1 in (3.14), we obtain, after integration by parts

$$\lambda^1 \int_{-\infty}^{\infty} \pi^0 \bar{u}_x = \pi^0 c \bar{u}_{xx}\big|_{-\infty}^{\infty} - \int_{-\infty}^{\infty} \pi^0 (b\bar{u}_x - c\bar{u}_{xxx}) - \int_{-\infty}^{\infty} \pi_x^0 c \bar{u}_{xx}.$$

Since the boundary terms vanish, the travelling wave ODE implies

$$\lambda^1 \int_{-\infty}^{\infty} \pi^0 \bar{u}_x = -\int_{-\infty}^{\infty} \pi^0 (f(\bar{u}) - f(u_-)) - \int_{-\infty}^{\infty} \pi_x^0 c \bar{u}_{xx}. \tag{3.18}$$

To proceed further, we have to determine the left eigenfunction, by finding a solution of (3.15) with the appropriate behaviour at $\pm\infty$.

The discussion of the boundary conditions for π^0 depends upon the growth/decay rate of the travelling wave and the first order correction of the left eigenfunction, and leads to different results for the compressive and the undercompressive case.

In the *Lax or compressive case, ($a_- > 0 > a_+$),* we have that the weight Ω of (3.6) grows exponentially. Thus, functions in L^2_Ω decay exponentially at $+\infty/-\infty$, while functions in $L^2_{\Omega^{-1}}$ are allowed to *grow* exponentially. Thus, the *constant solution* $\pi^0 \equiv \frac{1}{(u_+ - u_-)}$ of

$$L_0^* w = -(cw_x)_{xxx} + (bw_x)_x + aw_x = 0 \tag{3.19}$$

is the unique $L^2_{\Omega^{-1}}$ left eigenfunction, whereas $\bar{u}_x$ is the exponentially decaying right eigenfunction in L^2_Ω. (Note: $\langle \pi^0, \bar{u}_x \rangle = 1$). This validates the formal calculation in [THSJ89, BB97] via (3.13), which in this case is equivalent to simple integration, yielding

$$\lambda^1 = \int_{-\infty}^{\infty} \frac{f(u_-) - f(\bar{u})}{u_+ - u_-}\, dx. \tag{3.20}$$

In the *undercompressive case, ($a_-, a_+ < 0$),* on the other hand, Ω blows up as $x \to +\infty$ but *decays* as $x \to -\infty$. Thus, L^2_Ω functions may *grow* exponentially while $L^2_{\Omega^{-1}}$ functions must *decay* exponentially at $-\infty$. The latter fact implies that π^0 in this case is *not a*

constant function, hence the formal calculation of [THSJ89, BB97] no longer corresponds to (3.13).

Moreover, numerical computations by the *power method* reveal that φ^1 indeed grows exponentially as $x \to -\infty$. Thus, the calculation of the Lax case, by integration against a constant is *not valid* to test stability in the undercompressive case, the resulting integral being unbounded, hence the conclusion of instability by this test is false. (Of course, this fallacy would likewise be detected at the level of solving for φ^1.) This gives a simple explanation of the aforementioned long-wave paradox.

We further examine the growth rate of φ^1 at $-\infty$ analytically: the slow growth rate $\mu_-(k,\lambda)$ perturbing from the one-dimensional root $\mu_-(0,0) = 0$ of the characteristic equation for $L_{k_\pm}$,

$$-c_\pm\mu^4 + b_\pm\mu^2 - \mu a_\pm - c_\pm k^4 - k^2(b_\pm - 2c_\pm\mu^2) = \lambda \tag{3.21}$$

(analogous to the one-dimensional version (2.7)), at $k = 0, \lambda = 0$, gives

$$\mu_\pm(k,\lambda) = -\frac{(\lambda + b_\pm k^2)}{a_\pm}. \tag{3.22}$$

Now, let us consider the case $b \equiv 0$ corresponding to the stability computations of the undercompressive wave in [BMFC98]. Here, $\mu_- = -\lambda/a_- + H.O.T$. Thus, in the case of *stability*, $\lambda^1 < 0$, we have

$$\mu_-(k,\lambda(k)) \sim \mu_-(k,\lambda^1 k^2) \sim -\frac{\lambda^1 k^2}{a_-} < 0, \tag{3.23}$$

and so $\varphi(k)$ generically exhibits *exponential growth* as $x \to -\infty$ for any small $k > 0$, the exception arising when $\mathscr{S}^+$ intersects $\mathscr{U}^-$ precisely along the unique decaying solution corresponding to the remaining (positive) root. Indeed, $\varphi(k)$ (generically) decays at $\pm\infty$ in the case of *instability*!

Remark The growth of φ at $-\infty$ also raises an apparently subtle issue of competition between exponential temporal decay $e^{\mathrm{Re}\,\lambda(k)t}$ and exponential spatial *growth*, and indeed, this issue is not resolved by considerations in the Ω norm (where spatial growth is ignored at $-\infty$). However, heuristically, note that at the order of λ_1, the dominant linear behaviour in the far field at $-\infty$ is

$$e^{k^2\lambda_1 t}e^{-\lambda_1 k^2 x/a_-} = \exp\left(\frac{-\lambda_1 k^2}{a_-}(x - a_- t)\right)$$

which is precisely a translating wave with speed a_- and shape corresponding to the eigenfunction in the far field. Thus, the exponential growth of the eigenfunction and exponential decay of the eigenvalue combine to produce a translation in the far field. This is consistent with the fact that for the undercompressive wave, information passes through the waves and goes off to $-\infty$ with speed a_-. Preliminary numerical computations [M99] verify that, in this regime, temporal decay indeed wins out over spatial growth.

More detailed computations of [HoZ.3, Z.2], in the second order diffusive case, carry over in straightforward fashion to the case of higher-order diffusion (see [HZ.2] for a one-dimensional version) to reveal that

$(\mathscr{D}_k)$ $\operatorname{Re}\lambda(k) \leqslant \theta k^2, \quad \theta < 0$, for the largest eigenvalue $\lambda(k)$ of L_k

is a sufficient condition for linearized stability, independent of spatial growth of eigenfunction φ, or in our notation,

$$\lambda^1 < 0. \tag{3.24}$$

3.3 Alternative solvability condition

As discussed above, in the undercompressive case, $\pi^0 \equiv$ constant is *no longer a left eigenfunction* for $\overline{u}_x$ (as in the Lax case). Indeed, this is the key difference between Lax and undercompressive waves pointed out in [LZ.2]: the *shock shift* (represented at the linearized level by the component of instantaneous translation $\overline{u}_x$) is not determined by *mass* (i.e. projection $\langle 1, \cdot \rangle$), but by a different time-invariant of the solution $\langle \pi^0(\cdot), \cdot \rangle$, where π^0 is an nonconstant bounded solution of

$$L^* \pi^0 = 0, \tag{3.25}$$

with boundary conditions

$$\begin{cases} \pi^0(x) \to 1 & \text{as } x \to +\infty \\ \pi^0(x) \to 0 & \text{as } x \to -\infty. \end{cases} \tag{3.26}$$

The boundary conditions can be understood heuristically from the observation that mass near $+\infty$ is swept inward by convection $a_+ < 0$, to interact with the shock, while mass near $-\infty$ is swept away by $a_- < 0$, never affecting the shock (see [ZH, § 10], for a rigorous discussion). The condition at $+\infty$ may be deduced rigorously by consideration of growth/decay rates at $+\infty$ of solutions of the adjoint eigenvalue equation, which reveals that solutions in $L^2_{\Omega^{-1}}$ must in fact be bounded (note: growing solutions grow at too great an exponential rate). The condition at $+\infty$ is clear, by exponential decay of functions in $L^2_{\Omega^{-1}}$.

3.4 Numerical results

In this subsection, we describe numerical results for the thin film equation

$$u_t + \left(u^2 - u^3\right)_x = -\nabla \cdot \left(u^3 \nabla \Delta u\right), \tag{3.27}$$

which is equation (1.5) with $b = 0, \quad c = u^3, \quad f = u^2 - u^3$. We focus exclusively on the multi-dimensional stability of one-dimensional travelling waves. A preliminary stability analysis in [BMFC98] of compressive waves revealed that they were unstable against two-dimensional perturbations for a range of wavenumbers $k > 0$. On the other hand, the undercompressive wave was stable for all wavenumbers. These results agree with experimental observations of the liquid front.

In this paper, we calculate the critical growth rate $\lambda(k)$ for a variety of compressive and undercompressive travelling waves, and compare the results with the long-wave asymptotic result $\lambda(k) \sim \lambda^1 k^2$ as $k \longrightarrow 0+$, in which the coefficient is calculated numerically from the formulae above. There are several interesting features of the behaviour of $\lambda(k)$ for moderate k, linked to the presence of a countable family of compressive waves for the wave speed at which there is also an undercompressive wave.

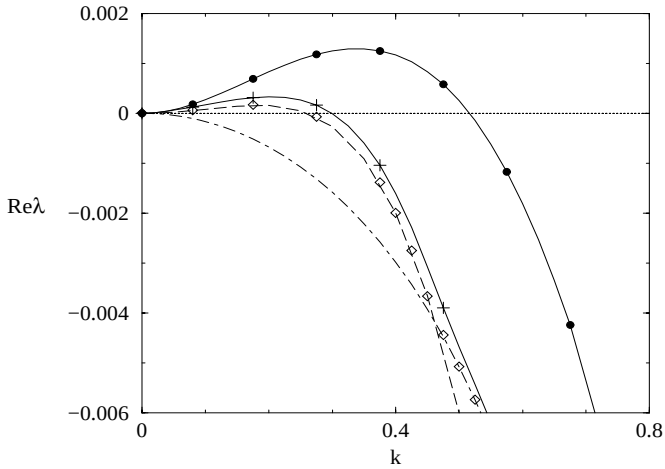

FIGURE 6. The stability curves for general k. The results for the three simple compressive waves are given by bullets, plus and diamonds. The curves for waves one and three are filled in by solid lines. For the *trailing* compressive wave, the stability curve is given by a dashed line, and a dot-dashed line for the undercompressive base profile.

3.4.1 *Computation of the largest eigenvalue using the power method*

For each of the travelling wave solutions, the values of the base profiles $\bar{u}$ on the finite difference grid are obtained by solving the travelling wave ODE, or by computing long-time solutions of the one-dimensional PDE. Then the dominant eigenvalue $\lambda(k)$ and the corresponding eigenfunction are obtained for various wavenumbers k by solving (3.2) numerically. As in [BB97, BMFC98], we used a finite difference scheme, with an implicit Euler time step to calculate $\hat{v}$, then extracted the eigenvalue from the time evolution of $\hat{v}$ after the exponential decay or growth rate in time had appeared. In addition, eigenvalues/functions were also confirmed by inverse vector iteration, a particularly useful method for computing subdominant or pairs of complex conjugate eigenvalues as in § 3.4.3.

We set parameters for the travelling waves by choosing $u_+ = 0.1$, $u_- = 0.332051$, and shift to a reference frame (by subtracting a linear term from the flux) so that the wave is stationary. For this choice of parameters, we find an infinite number of travelling wave solutions, as observed in [BMS99], but, as discussed in § 2.5, only every other one is stable as a solution of the *one-dimensional* version of (3.27). For the same parameters, there are two additional travelling waves: an undercompressive wave, from $u_T \equiv 1 - u_- - u_+ = 0.567949$ to u_+, and a trailing compressive wave from u_- to u_T. (The latter wave is termed *trailing* because it corresponds to compressive waves that trail the undercompressive wave in numerical simulations [BMS99] of the partial differential equation with a certain range of initial data, in the limit that the two wave speeds coincide.)

Figure 6 shows stability curves (graphs of $\lambda = \lambda(k)$) for three of the compressive waves from u_- to u_+ (the first three in the ordering of [BMS99] that are stable to one-dimensional perturbations), for the undercompressive wave and for the trailing wave. The results for

the first and third travelling wave are shown by solid lines, with additional symbols (bullets, pluses and diamonds) for the first, third and fifth travelling waves. A dot-dash curve represents the eigenvalue for the undercompressive wave, and a dashed curve the trailing compressive wave. We do not use a solid line for the fifth compressive wave, since it would coincide with the undercompressive and trailing compressive wave curves. From the figure, we immediately observe that the compressive waves all have a range of $k > 0$ for which they are unstable, whereas the undercompressive profile is linearly stable against transverse perturbations.

Figure 6 also shows the following interesting phenomenon. Let $\lambda(k;i)$ denote the stability curve for the $(2i-1)$th travelling wave (recall that the even numbered waves are unstable to one dimensional perturbations), and let $\lambda_{uc}(k)$ and $\lambda_{tr}(k)$ denote the dominant eigenvalues for the undercompressive and trailing compressive waves, respectively. In Figure 6, observe that the graphs of $\lambda(k;3)$ and of $\max\{\lambda_{uc}(k), \lambda_{tr}(k)\}$ are virtually indistinguishable. This observation suggests that

$$\lim_{i\to\infty} \lambda(k;i) = \max\{\lambda_{uc}(k), \lambda_{tr}(k)\}. \tag{3.28}$$

This unusual limiting behaviour may be understood as follows: for large i, the $(2i-1)$th travelling wave has a well-separated leading and trailing front which closely resembles a double shock composed of a leading undercompressive shock, and a trailing compressive shock having the same speed, each of which have travelling wave profiles. Correspondingly, the compressive travelling wave trajectories in phase space (i.e. trajectories from the middle equilibrium M to the bottom equilibrium B) are approximated by the union of a trajectory from M to T of the trailing compressive wave and the trajectory from T to B of the undercompressive trajectories at these parameter values. Hence the eigenvalues for these approximately composite waves are approximately given by the union of the eigenvalues of the component undercompressive and trailing waves. These general principles are familiar from the study of multi-hump solitary wave solutions in the reaction–diffusion and nonlinear optics literature, [AJ1, AGJ1, L, S.1, S.2].

Though the proofs (from the solitary wave theory) in general break down for systems of conservation laws, due to the lack of a spectral gap at $\lambda = 0$, in the present, scalar setting they can be applied unchanged, after the usual weighting transformation to recover a spectral gap. (Alternatively, one could recall from § 2.2 the fact that $\mathscr{S}^+$ and $\mathscr{U}^-$ remain spectrally separated at $k = 0$, $\lambda = 0$, and carry out a direct proof using Evans function methods. These issues are discussed in [Z.3].)

Likewise, the eigenfunctions tend to be superpositions of the eigenfunctions (shifted so they essentially do not overlap, in keeping with the trajectories themselves) of the undercompressive and trailing compressive waves. The growth rate of the composition is then governed by the maximum of the growth rates of each part.

This observation suggests the following property:

At $k = k_1$, where the two stability curves $\lambda_{uc}(k)$, $\lambda_{tr}(k)$ intersect, we might expect a loss of smoothness in $\lambda(k;i)$ for $i \to \infty$, and possibly for large enough finite i. The behaviour near $k = k_1$ is explored further in § 3.4.3.

3.4.2 *Comparison with long-wave asymptotics*

Next, we examine the range $0 < k < 0.1$ in greater detail, and compare $\lambda(k)$ for each compressive wave with the asymptotic form $\lambda^1 k^2$, the coefficients λ^1 being calculated separately for each wave from the formula (3.20). The results are shown in the log-log plot of Figure 7 (left). In this figure, symbols correspond to computed values of $\lambda(k)$ with triangles for the trailing wave, and circles, pluses and diamonds for waves one, three and five, respectively. The times symbols on the right are for the undercompressive wave. The solid lines represent $\lambda^1 k^2$ for compressive waves one and three. The line for wave five is indistiguishable from that for wave three. The dashed line represents $\lambda^1 k^2$ for the trailing wave, and the dot-dashed line for the undercompressive wave.

In Figure 7 (left), we note that the graphs of $\lambda(k;i), i = 1,2$ clearly approach the asymptotic curves as $k \to 0$, and stay reasonably close throughout the range $0 < k < 0.1$. However, the graph of $\lambda(k,3)$ switches over in this range of k from the asymptotic curve to the curve for the compressive trailing wave. We conclude the following property: Figure 7 (left) suggests that the coefficient λ_i^1 for the $(2i-1)$th compressive travelling wave has a limit, and that

$$\lim_{i\to\infty} \lambda_i^1 \neq \lambda_{tr}^1.$$

Moreover, the numerics suggest that for larger i, the leading order long-wave asymptotics agrees with the spectrum for a smaller range of k near zero. We conjecture that the analytic expansion breaks down in the limit as $k \to \infty$ where we are essentially linearizing about a composite wave.

For the undercompressive wave, the linear stability analysis for general k can be done with the same numerical method as for the compressive case. To compute the coefficient of the long wave expansion λ^1, we have to start with (3.18), and use the non-constant eigenfunction π^0 satisfying (3.15) with boundary conditions (3.26). Note that the argument presumes that $\lambda^1 < 0$, which can, in part, be justified here by referring to the numerical results for general k.

The adjoint problem (3.15), (3.26) was solved by discretizing the equation with finite differences similar as for the general-k problem, then solving for π^0 iteratively in a process similar to the iterative vector-iteration process used to calculate eigenvectors for known eigenvalues [Ke, PTVF]. Specifically, let $p = (p_i)$, $i = 1 \ldots N$ denote the vector of grid-values approximating π^0, and L_{disc} the discrete $N \times N$-matrix representation of the continuous operator given by (3.15), and the discrete boundary conditions

$$p_0 = p_2 - 2p_1 + p_0 = 0, \qquad p_n - p_{n-1} = p_n - 2p_{n-1} + p_{n-2} = 0. \tag{3.29}$$

Then, successive approximations to π^0 are obtained by solving

$$p_{new} := \frac{L_{disc}^{-1} p_{old}}{||L_{disc}^{-1} p_{old}||_\infty},$$

where $||-||_\infty$ denotes the discrete maximum norm. Note that, even though L_0^* is singular, the spectrum of the discretized operator will typically not include the eigenvalue zero, i.e. this operator is invertible and the above step can be carried out. After very few iterations, in fact we found in our numerical trials after the first iteration, the sequence of discrete p becomes stationary. The vector thus obtained is an eigenvector for the eigenvalue with

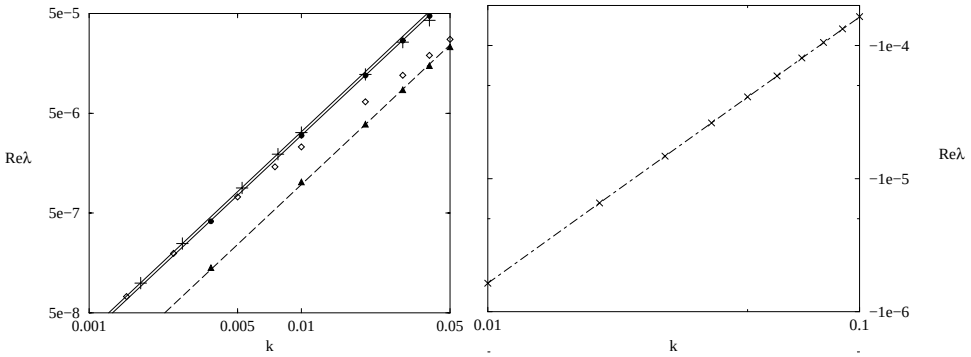

FIGURE 7. (Left) Stability curves for the compressive profiles for small k in a log-log plot. The symbols (circles, pluses, diamonds) represent the numerically calculated $\lambda(k)$ (for the first, third and fifth waves, respectively). Solid lines show the $\lambda^1 k^2$ for waves one, three and five. The dashed line shows $\lambda^1 k^2$ for the trailing wave. (Right) Stability curve for the undercompressive shock. Symbols denote the values computed for $\lambda(k)$ using the code for general k, the dot-dashed line represents the long-wave approximation.

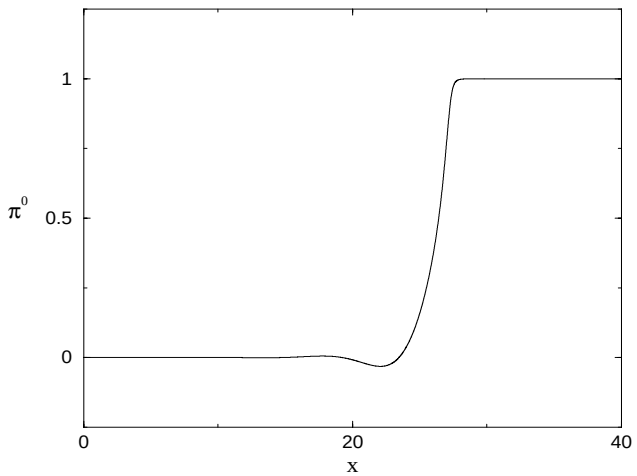

FIGURE 8. The non-constant left eigenfunction for the undercompressive profile.

the smallest modulus, and hence a good approximation of π^0. For the special situation of equation (3.27), the resulting $\pi^0(x)$ is shown in Figure 8. Note that the choice (3.29) for the discrete boundary conditions excludes convergence to a constant solution.

This π^0 is then used to evaluate (3.18). The resulting plot for $\lambda^1 k^2$ is shown in Figure 7 (right) as a dot-dashed line. The agreement with the numerical values $\lambda(k)$ is excellent.

3.4.3 *The spectrum for higher order compressive waves*

We now present some more detailed computations showing the structure of the higher order compressive waves. Using an iterative method similar to that used to compute π^0, we can compute the largest *two* eigenvalues of the linearized operator corresponding to travelling waves three ($i = 2$) and five ($i = 3$).

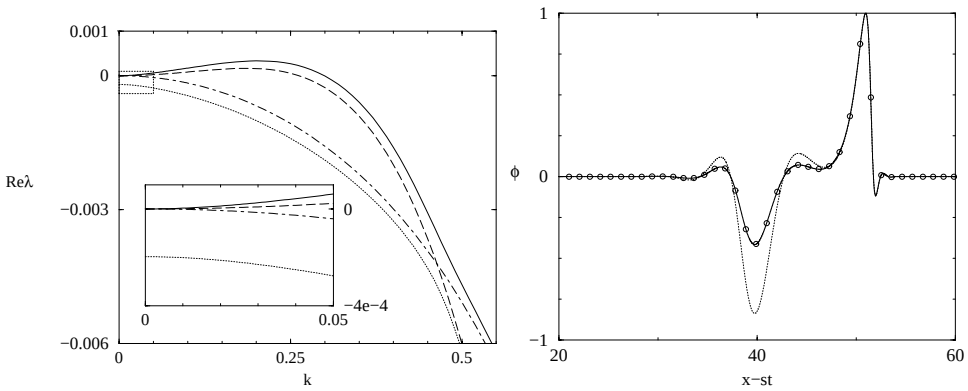

FIGURE 9. (Left) Spectrum of the first two eigenvalues (shown as solid and dotted lines) for the third compressive wave ($i = 2$). The dot-dashed line and long-dashed line show the dominant eigenvalue for the undercompressive wave and trailing wave, respectively. The inset is an enlarged view of a region near $k = 0$, marked by a box with dotted lines in the outer graph. (Right) The eigenfunctions for the first two eigenvalues of travelling wave three ($i = 2$) at $k = 0$.

Figure 9 shows the largest two eigenvalues and corresponding eigenfunctions for wave number three ($i = 2$). On the left, the solid line shows the largest eigenvalue and the dotted line shows the second eigenvalue. The long-dashed line shows the dominant eigenvalue for the trailing wave and the dot-dashed line the dominant eigenvalue for the undercompressive wave. It is clear for travelling wave three that the two eigenvalues are well separated, and that the second eigenvalue approaches a small but negative value as $k \to 0$. On the right are the eigenfunctions for the largest two modes at $k = 0$. The eigenfunction with $\lambda = 0$ is shown as the solid line; it agrees precisely with the translation mode u_x shown via circles. The eigenfunction corresponding to the negative eigenvalue is shown via a dotted line; it corresponds to infinitesimal but unequal shifts of the leading and the trailing edges of the wave, indicated by the observation that this wave is approximately cu_x for $c > 1$ near the trailing part of the wave and u_x near the leading part of the wave. The small negative value of this eigenvalue at $k = 0$ reflects the fact that the wave is just stable against one-dimensional perturbations towards one of its neighboring waves.

Figure 10 shows the largest two eigenvalues and corresponding eigenfunctions for wave number five ($i = 3$). On the left, the solid line shows the largest eigenvalue and the dotted line shows the second eigenvalue. The long-dashed line showing the dominant eigenvalue for the trailing wave and the dot-dashed line the dominant eigenvalue for the undercompressive wave are only shown in the inset, as their agreement with the largest two eigenvalues of wave number five is very good. Unlike travelling wave three, the two eigenvalues of travelling wave five are not well separated, and appear to cross in the region marked with a box and blown up in Figure 11. However, as for travelling wave three, the second eigenvalue approaches a small but negative value as $k \to 0$. The inset shows an enlarged view of a region near $k = 0$, delineated, in the outer graph, by a small box with dotted lines. For a blow-up of the region near $k = k_1$ marked by the larger box with *solid* lines (see figure 11).

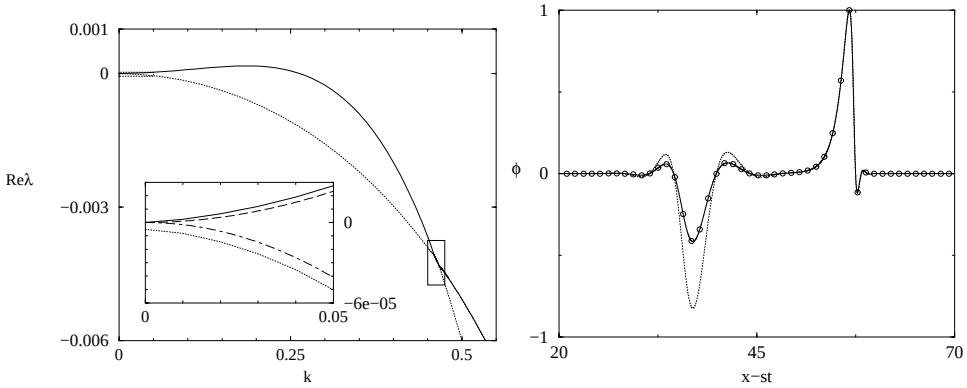

FIGURE 10. (Left) Spectrum of first two eigenvalues (shown as solid and dotted lines) for the fifth ($i = 3$) compressive wave. The dot-dashed line and long-dashed line in the inset show the dominant eigenvalue for the undercompressive wave and trailing wave, respectively. (Right) The eigenfunctions for the first two eigenvalues of travelling wave five ($i = 3$) at $k = 0$.

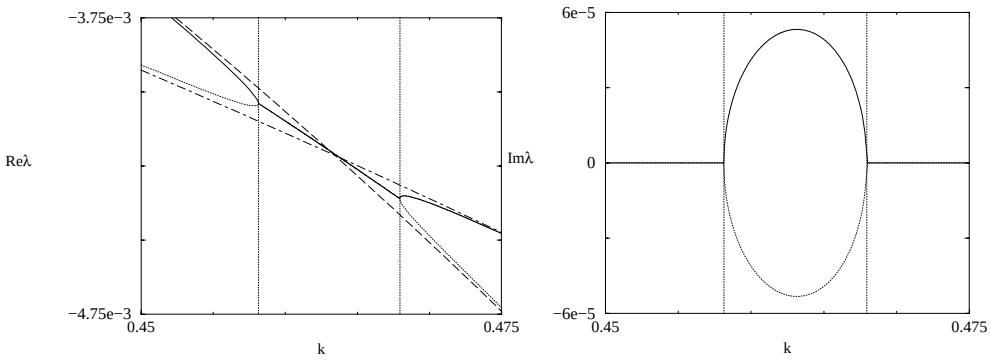

FIGURE 11. (Left) Enlarged view of the real part of the first two eigenvalues (shown as solid and dotted lines) for the fifth compressive wave. The dot-dashed line and long-dashed line show the dominant eigenvalue for the undercompressive wave and trailing wave, respectively. (Right) The imaginary part of the eigenvalues shown on the left.

On the right are the eigenfunctions for the largest two modes at $k = 0$. The eigenfunction with $\lambda = 0$ is shown as the solid line; again, it agrees precisely with the translation mode u_x shown via circles. The eigenfunction corresponding to the negative eigenvalue is shown via a dotted line; it again corresponds to infinitesimal but unequal shifts of the leading and the trailing edges of the wave.

Figure 11 shows an enlarged view of $\mathrm{Re}\,\lambda(k)$ and $\mathrm{Im}\,\lambda(k)$ near the point where the two eigenvalues appear to cross in Figure 10. The line styles carry over from that figure. As k approaches the intersection point, the largest and second eigenvalues coalesce, giving rise to a complex conjugate pair of eigenvalues, which reseparate into real eigenvalues after the intersection point. The imaginary part of the eigenvalues is shown to grow from zero and then shrink back to zero during this transition (see right figure). The vertical dotted lines on each graph have exactly the same k values, and delineate the bifurcation points in k.

4 Conclusions

In summary, we have explored the stability of traveling waves in thin films driven by gravity and surface-tension gradients. We develop an Evans function theory for the one-dimensional stability of traveling waves that applies to a general class of viscous conservation laws including the thin film equations. In higher dimensions we develop a long-wave asymptotic theory for both compressive and undercompressive traveling waves. The results are reinforced by numerical simulations.

In the context of thin films, it is interesting that the phase portrait geometry underlying the existence of multiple traveling waves is encoded in the stability index Γ (2.6). In [BMS99], we presented numerical evidence showing a cascade of bifurcations in the compressive traveling wave problem as the shock speed varies. In particular there exists a range of values of the shock speed for which there are multiple compressive waves with the same speed, left state, and right state. For a special shock speed there exists a countable infinity of such waves. We observed numerically that when multiple waves are ordered according to their relative position along the unstable manifold of the middle equilibrium in the phase portrait for the traveling wave problem, that these waves alternate stability in one-dimension. In this paper, we explain this observation by noting that the stability index Γ necessarily alternates sign, since its sign depends upon the orientation of the stable and unstable manifolds in the traveling wave phase portrait, as shown in Figure 4. This provides a proof of instability for the even numbered waves, and consistency with stability of the odd numbered waves. An example of the profiles of such traveling waves is shown in Figure 2.

An important discovery for driven films is that undercompressive waves exist at a special value of the shock speed. For the undercompressive wave, we derive a new formula (2.55) for the one-dimensional stability index that can be calculated numerically.

In §3 we consider the stability of traveling waves to transverse perturbations. For compressive waves that are one-dimensionally stable, we provide a rigorous justification for a long-wave asymptotic formula first derived by Troian *et al.* [THSJ89]) for flow down a vertical plane. This is formula (3.20) for the leading order behavior ($\lambda^1 k^2$) of the largest eigenvalue in the small wave number limit ($k \to 0$). We discover, however, that this formula is not valid for undercompresive waves. This 'long-wave paradox' is resolved by the observation that, for the undercompressive wave, the eigenfunction for the zero eigenvalue of the adjoint linearized equation has spatial dependence, unlike the compressive case, for which it is constant. Taking this into account results in a new expression for the asymptotics for undercompressive waves, implying that they are stable to long wave transverse perturbations. An interesting feature of the dominant eigenfunction (for the linearized equation) is that, for small positive values of the wavenumber k, it has spatial exponential growth at $-\infty$.

Finally, we examine the k-dependent spectrum for higher order compressive waves, as in the case of waves numbered three and five in Figure 2. These waves are approximations of a composite wave comprised of the undercompressive wave in front and a trailing compressive wave behind it. We show via numerical computations that the largest eigenvalue for the higher order waves is well approximated by the maximum of the eigenvalues for the respective undercompressive and trailing compressive waves. The structure of the

spectrum near the cross-over point can develop nonzero imaginary parts, as shown in Figure 11.

We emphasize that, while this paper explores stability questions in some detail, our understanding of stability is still quite primitive. For example, we do not attempt to analyze the Evans function in its entirety, and our analytical results on stability to transverse perturbations are confined to small wave number asymptotics. Numerical results provide a more complete assessment of stability. The problem discussed here is just one illustration of the rich structure of nonlinear fourth order PDEs and their connection to problems in thin liquid films.

Acknowledgements

We thank Tom Witelski for helpful discussions on the use of vector iteration for computing discrete eigenvalues of differential operators.

AM acknowledges support from ONR grant number N00014-96-1-0656 while at Duke and the support of the Center for Mathematics at the Technical University of Munich. He thanks Prof. Hoffmann and Prof. Brokate for encouraging his visits to Duke, and for providing access to up-to-date work-stations for the numerical computations.

References

[AJ1] Alexander, J. C. & Jones, C. K. R. T. (1994) Existence and stability of asymptotically oscillatory double pulses. *J. Reine Angew. Math.* **446**, 49–79.

[AGJ1] Alexander, J. C., Gardner, R. & Jones, C. K. R. T. (1990) A topological invariant arising in the stability analysis of travelling waves. *J. Reine Angew. Math.* **410**, 167–212.

[AGJS] Alexander, J. C., Grillakis, M. N., Jones, C. K. R. T. & Sandstede, B. (1997) Stability of pulses on optical fibers with phase-sensitive amplifiers. *Z. Ang. Math. Phys.* **48**, 175–192.

[BB97] Bertozzi, A. L. & Brenner, M. P. (1997) Linear stability and transient growth in driven contact lines. *Phys. Fluids* **9**(3), 530–539.

[BMFC98] Bertozzi, A. L., Münch, A., Fanton, X. & Cazabat, A. M. (1998) Contact line stability and 'undercompressive shocks' in driven thin film flow. *Phys. Rev. Lett.* **81**(23), 5169–5172.

[BMS99] Bertozzi, A. L., Münch, A. & Shearer, M. (1999) Undercompressive shocks in thin film flow. *Physica D*. **134**, 431–464.

[BS99] Bertozzi, A. L. & Shearer, M. (2000) Existence of undercompressive travelling waves in thin film equations, 1999. *SIAM J. Math. Anal.* **32**(1), 194–213.

[Br] Brin, L. (1998) Numerical Testing of Stability of Viscous Shock Waves. Doctoral Thesis.

[CC92] Carles, P. & Cazabat, A. M. (1992) On the origin of the bump in the profile of surface–tension–gradient–driven spreading films. *Mat. Res. Soc. Symp. Proc.* **248**.

[CHTC90] Cazabat, A. M., Heslot, F., Troian, S. M. & Carles, P. (1990) Finger instability of this spreading films driven by temperature gradients. *Nature*, **346**(6287), 824–826.

[CE] Collet, P. & Eckmann, J.-P. (1990) *Instabilities and Fronts in Extended Systems.* Princeton University Press, Princeton, NJ.

[D] Dodd, J. (1995) Stability of dispersive undercompressive shock waves. PhD thesis, University of Maryland.

[E] Evans, J. W. (1972–1975) Nerve axon equations: I–IV. *Ind. Univ. Math. J.* **21** (1972), 877–885; **22** (1972), 75–90; **22** (1972), 577–593; **24** (1975), 1169–1190.

[FH94] Fraysse, N. & Homsy, G. M. (1994) An experimental study of rivulet instabilities in centrifugal spin coating of viscous Newtonian and non-Newtonian fluids. *Phys. Fluids* **6**(4), 1491–1504.

[GJ.1] Gardner, R. & Jones, C. K. R. T. (1991) A stability index for steady state solutions of boundary value problems for parabolic systems. *J. Diff. Eqs.* **91**(2), 181–203.

[GJ.2] Gardner, R. & Jones, C. K. R. T. (1989) Traveling waves of a perturbed diffusion equation arising in a phase field model, *Ind. Univ. Math. J.* **38**(4), 1197–1222.

[GZ] Gardner, R. & Zumbrun, K. (1998) The gap lemma and geometric criteria for stability of viscous shock waves. *Comm. Pure Appl. Math.* **51**(7), 797–855.

[G] Goodman, J. (1989) Stability of viscous scalar shock fronts in several dimensions. *Trans. Amer. Math. Soc.* **311**(2), 683–695.

[GM] Goodman, J. & Miller, J. R. (1999) Long-time behaviour of scalar viscous shock fronts in two dimensions. *J. Dynam. Differential Equations* **11**(2), 255–277.

[Gre78] Greenspan, H. P. (1978) On the motion of a small viscous droplet that wets a surface. *J. Fluid Mech.* **84**, 125–143.

[GH] Guckenheimer, J. & Holmes, P. (1983) *Nonlinear Oscillations, Dynamical Systems, and Bifurcations of Vector Fields.* Applied Mathematical Sciences, **42**. Springer-Verlag.

[He] Henry, D. (1981) *Geometric Theory of Semilinear Parabolic Equations.* Lecture Notes in Mathematics, **840**. Springer-Verlag.

[HoZ.3] Hoff, D. & Zumbrun, K. (2001) Pointwise Green's function estimates for multi-dimensional scalar shock fronts. In preparation.

[HoZ.4] Hoff, D. & Zumbrun, K. (2001) Decay and asymptotic behavior of perturbed scalar shock fronts. *Indiana Univ. Math. J.* (to appear).

[H.1] Howard, P. (1998) Pointwise estimates for the stability of a scalar conservation law. Thesis, Indiana University.

[H.2] Howard, P. (1999) Pointwise estimates on the Green's function for a scalar linear convection–diffusion equation. *J. Differential Equations* **155**(2), 327–367.

[H.3] Howard, P. (1999) Pointwise Green's function approach to stability for scalar conservation laws. *Comm. Pure Appl. Math.* **52**(10), 1295–1313.

[HZ.2] Howard, P. & Zumbrun, K. (2001) Pointwise estimates and stability for dispersive-diffusive shock waves. *Arch. Rat. Mech. Anal.* (to appear).

[Hup82] Huppert, H. (1982) Flow and instability of a viscous current down a slope. *Nature*, **300**, 427–429.

[IMP] Isaacson, E., Marchesin, D. & Plohr, B. (1990) Transitional waves for conservation laws. *SIAM J. Math. Anal.* **21**, 837–866.

[JMS] Jacobs, D., McKinney, W. & Shearer, M. (1995) Travelling wave solutions of the modified Korteweg-deVries-Burgers equation, *J. Diff. Eq.* **116**, 448–467.

[JdB92] Jerrett, J. M. & de Bruyn, J. R. (1992) Finger instability of a gravitationally driven contact line. *Phys. Fluids A*, **4**(2), 234–242.

[J] Jones, C. K. R. T. (1983) Some ideas in the proof that the FitzHugh–Nagumo pulse is stable. *Nonlinear Partial Differential Equations* (Durham, NH, 1982), 287–292. (*Contemp. Math.* **17**, *Amer. Math. Soc.* Providence, RI. 1983)

[J1] Jones, C. K. R. T. (1984) Stability of the travelling wave solution of the FitzHugh–Nagumo system. *Trans. Amer. Math. Soc.* **286**(2), 431–469.

[JGK] Jones, C. K. R. T., Gardner, R. A. & Kapitula, T. (1993) Stability of travelling waves for non-convex scalar viscous conservation laws. *Commun. Pur. Appl. Math.* **46**, 505–526.

[K.1] Kapitula, T. (1991) Stability of weak shocks in λ–ω systems. *Indiana Univ. Math. J.* **40**(4), 1193–1112.

[K.2] Kapitula, T. (1994) On the stability of travelling waves in weighted L^∞ spaces. *J. Diff. Eq.* **112**(1), 179–215.

[K.3] Kapitula, T. (1997) Multidimensional stability of planar travelling waves. *Trans. Amer. Math. Soc.* **349**(1), 257–269.

[KS] Kapitula, T. & Sandstede, B. (1998) Stability of bright solitary-wave solutions to perturbed nonlinear Schrodinger equations. *Phys. D*, **124**, 58–103.

[KT97] Kataoka, D. E. & Troian, S. M. (1997) A theoretical study of instabilities at the advancing front of thermally driven coating films. *J. Coll. Int. Sci.* **192**, 350–362.

[KT98] Kataoka, D. E. & Troian, S. M. (1998) Stabilizing the advancing front of thermally driven climbing films. *J. Coll. Int. Sci.* **203**, 335–344.

[K] Kato, T. (1985) *Perturbation theory for linear operators*. Springer–Verlag.

[Ke] Kelley, C. T. (1995) *Iterative methods for linear and nonlinear equations*. SIAM, Philadelphia.

[KH75] Kopell, N. & Howard, L. N. (1975) Bifurcations and trajectories joining critical points. *Advances in mathematics*, **18**, 306–358.

[LP] Lax, P. D. & Phillips, R. S. (1978) Scattering theory for domains with non-smooth boundaries. *Arch. Rational Mech. Anal.* **68**, 93–98.

[L] Lin, X.-B. (1996) Asymptotic expansion for layer solutions of a singularly perturbed reaction-diffusion system. *Trans. Amer. Math. Soc.* **348**, 713–753.

[LZ.1] Liu, T.-P. & Zumbrun, K. (1995) Nonlinear stability of an undercompressive shock for complex Burgers equation. *Comm. Math. Phys.* **168**, 163–186.

[LZ.2] Liu, T.-P. & Zumbrun, K. (1995) On nonlinear stability of general undercompressive viscous shock waves. *Comm. Math. Phys.* **174**, 319–345.

[LL] Ludviksson, V. & Lightfoot, E. N. (1971) The dynamics of thin liquid films in the presence of surface-tension gradients. *Am. Inst. Chem. Eng. J.* **17**(5), 1166–1173.

[M99] Münch, A. (2000) Shock transitions in Marangoni-gravity driven thin film flow. *Nonlinearity* **13**, 731-746.

[MB99] Münch, A. & Bertozzi, A. L. (1999) Rarefaction-undercompressive fronts in driven films. *Physics of Fluids*, **11**(10).

[MW99] Münch, A. & Wagner, B. (1999) Numerical and asymptotic results on the linear stability of a thin film spreading down a slope of small inclination. *Euro. J. Appl. Math.* **10**, 297–318.

[PW] Pego, R. L. & Weinstein, M. I. (1992) Eigenvalues, and instabilities of solitary waves. *Phil. Trans. R. Soc. London Ser. A*, **340**(1656), 47–94.

[PTVF] Press, W. H., Teukolsky, S. A., Vetterling, W. T. and Flannery, B. P. (1992) *Numerical Recipes in C: the Art of Scientific Computing*. Cambridge University Press, Second ed.

[P] Promislow, K. Preprint on stability of optical pulses.

[Ren96] Renardy, M. (1996) A singularly perturbed problem related to surfactant spreading on thin films. *Nonlinear Analysis, Theory, Methods, Applications*, **27**(3), 287–296.

[S.1] Sattinger, D. H. (1977) Weighted norms for the stability of traveling waves. *J. Diff. Eq.* **25**, 130–144.

[S.2] Sattinger, D. H. (1976) On the stability of waves of nonlinear parabolic systems. *Advances in Math.* **22**, 312–355.

[Sch] Schecter, S. (1987) The saddle-node separatrix-loop bifurcation. *SIAM J. Math. Anal.* **18**, 1142–1156.

[SSch] Shearer, M. & Schecter, S. (1991) Transversality for undercompressive shocks in Riemann problems. In: M. Shearer, editor, *Viscous Profiles and Numerical Methods for Shock Waves*. SIAM, 209–236.

[SV85] Silvi, N. & Dussan V, E. B. (1985) On the rewetting of an inclined solid surface by a liquid. *Physics of Fluids* **28**, 5–7.

[Sl] Slemrod, M. (1983) Admissibility criteria for propagating phase boundaries in a van der Waals fluid. *Arch. Rat. Mech. Anal.* **81**, 301–315.

[THSJ89] Troian, S. M., Herbolzheimer, E., Safran, S. A. & Joanny, J. F. (1989) Fingering instabilities of driven spreading films. *Europhys. Lett.* **10**(1), 25–30.

[TWS89] Troian, S. M., Wu, X. L. & Safran, S. A. (1989) Fingering instabilities in thin wetting films. *Phys. Rev. Letters*, **62**(13), 1496–1499.

[W] Wu, C. C. (1991) New theory of MHD shock waves. In M. Shearer, editor, *Viscous Profiles and Numerical Methods for Shock Waves*. SIAM, 209–236.

[YC99] Ye, Y. & Chang, H.-C. (1999) A spectral theory for fingering on a prewetted plane. *Physics of Fluids*, **11**(9), 2494–2515.

[Y] Yosida, K. (1995) *Functional Analysis*. Classics in Mathematics. Springer-Verlag.

[Z.2] Zumbrun, K. (1999) Multi-dimensional stability of viscous shock waves. *TMR summer school notes*. Köchel am See meeting.

[Z.3] Zumbrun, K. (1998) Stability of viscous shock waves. Indiana University lecture notes.

[ZH] Zumbrun, K. & Howard, P. (1998) Pointwise semigroup methods and stability of viscous shock waves. *Indiana Univ. Math. J.* **47**(3), 741–871.

[ZS] Zumbrun, K. & Serre, D. (1999) Viscous and inviscid stability of multi-dimensional planar shock fronts. *Indiana Math. J.* **48**(3), 937–992.

[Z.note] Zumbrun, K. (1998) Calculation of scattering coefficients for transitional shock waves. Unpublished note.